Figures

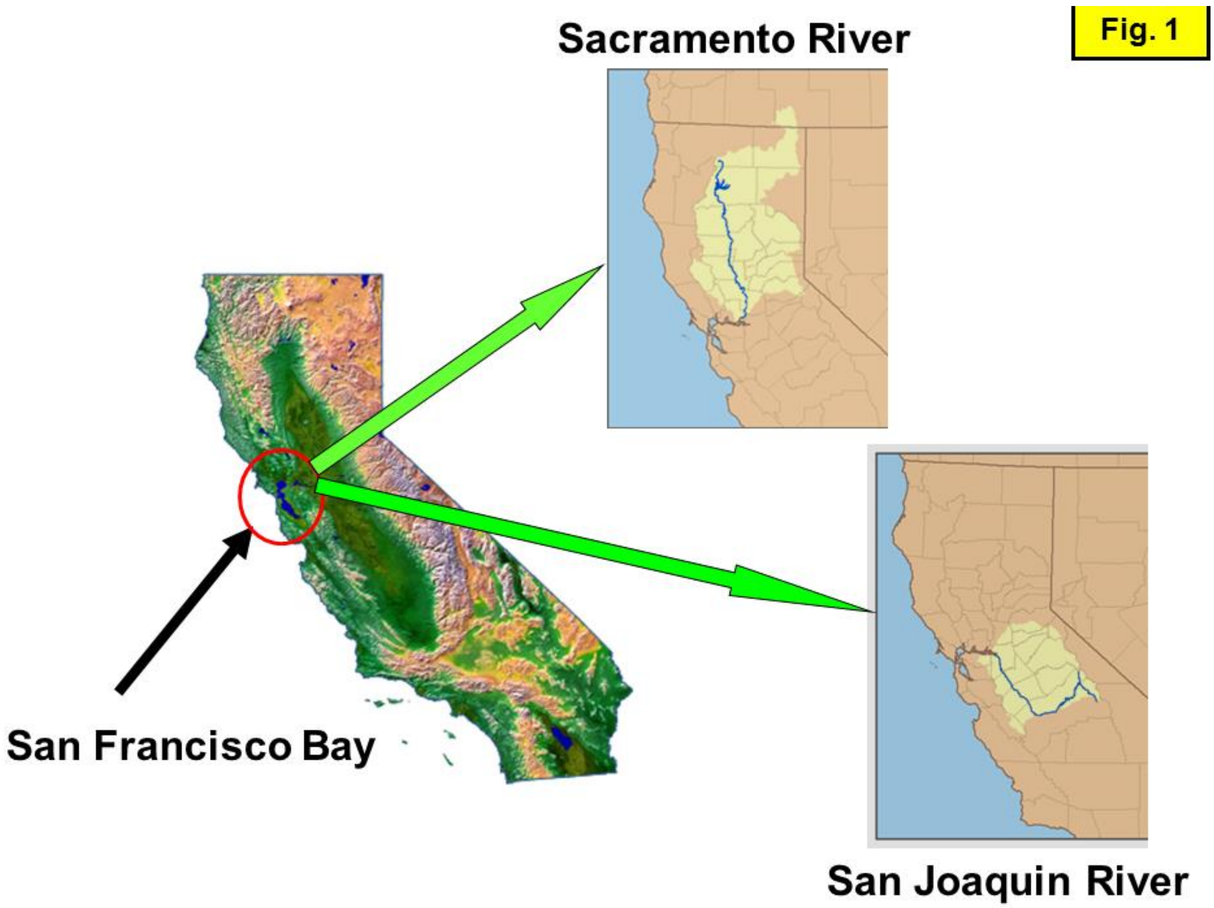

Figure 1
The San Francisco Estuary (SFE) drains the two major rivers in California, the higher-flow Sacramento River and the San Joaquin River. These rivers drain the main agricultural basins in the Central Valley, and both have major WWTPs at the upstream ends of the tidal parts of the rivers.

Fig. 2

Locations of sampling sites

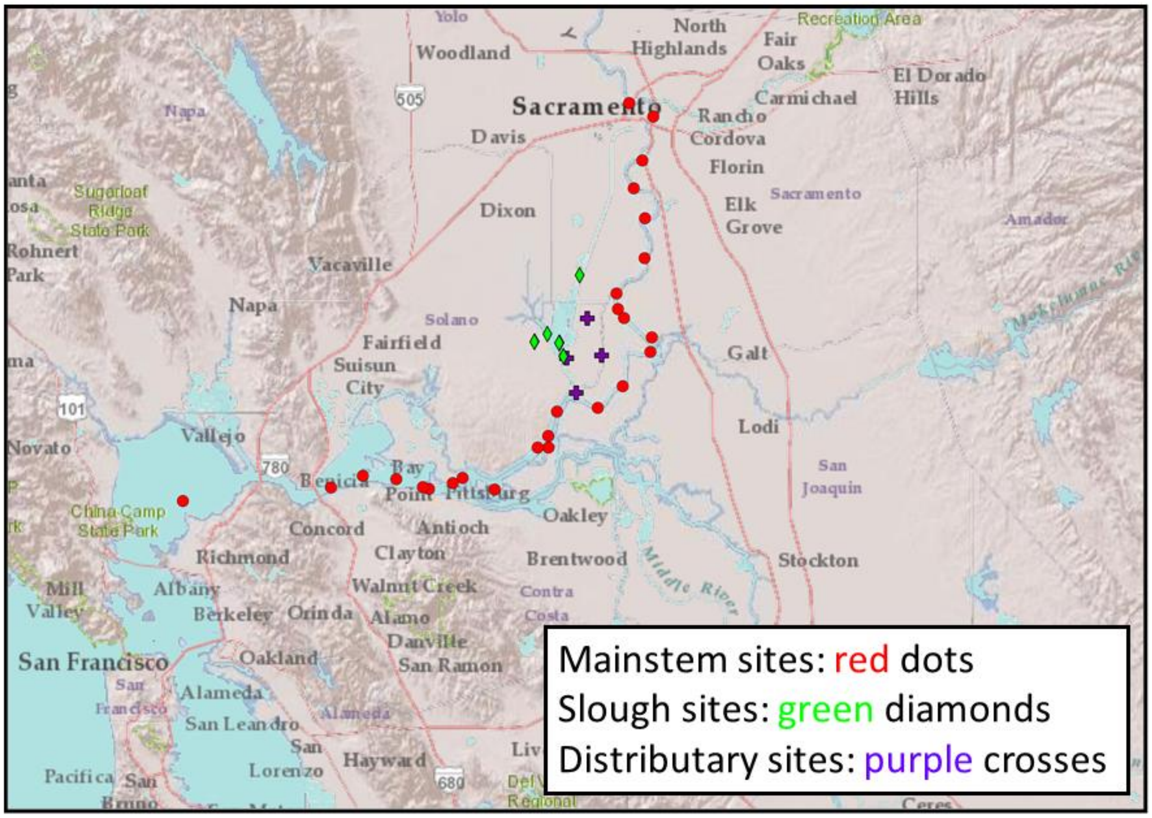

Figure 2

This map shows the location of sampling sites in the Sacramento River, Delta, northern San Francisco Bay, with different symbols for the different types of sites: mainstem, slough, and distributary.

Locations and names of mainstem sampling sites

Fig. 3

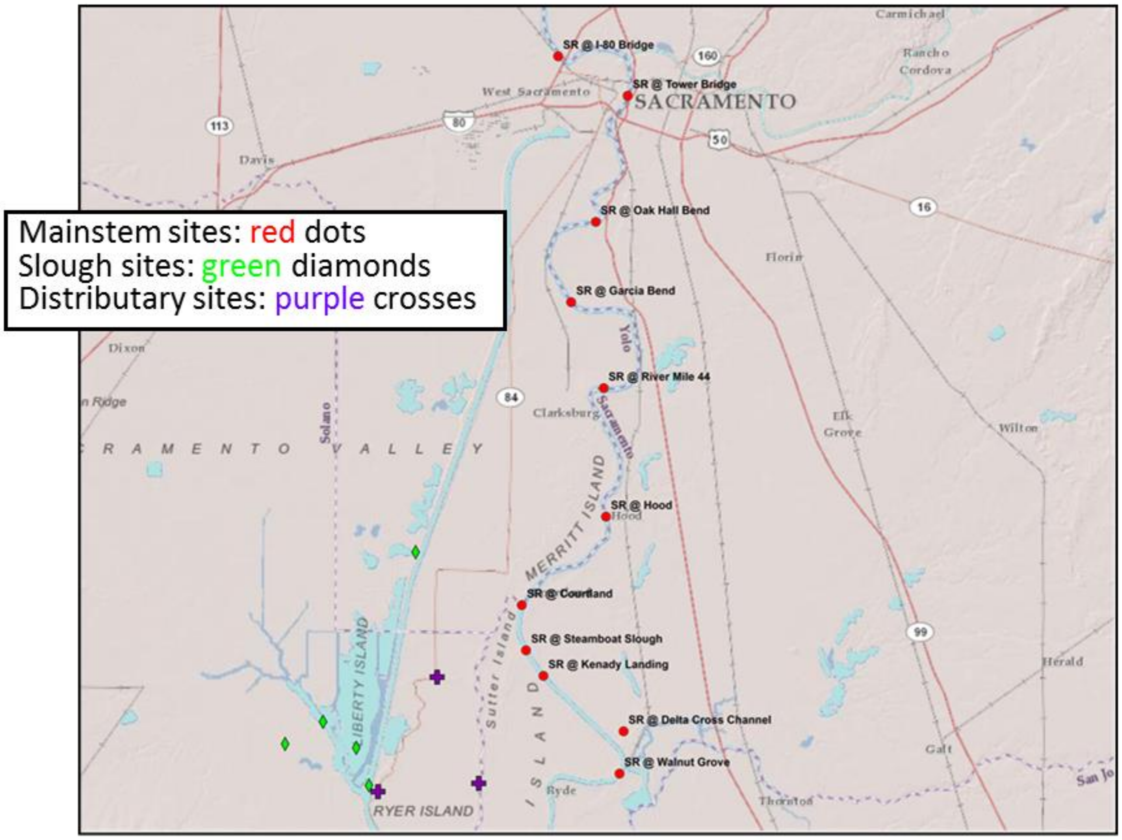

[Figure 3](#)
This map is an expanded version of **[Figure 2](#)** that includes the site names for sampling sites on the **mainstem** Sacramento River; see Table 1 for more information about the sites.

Fig. 4

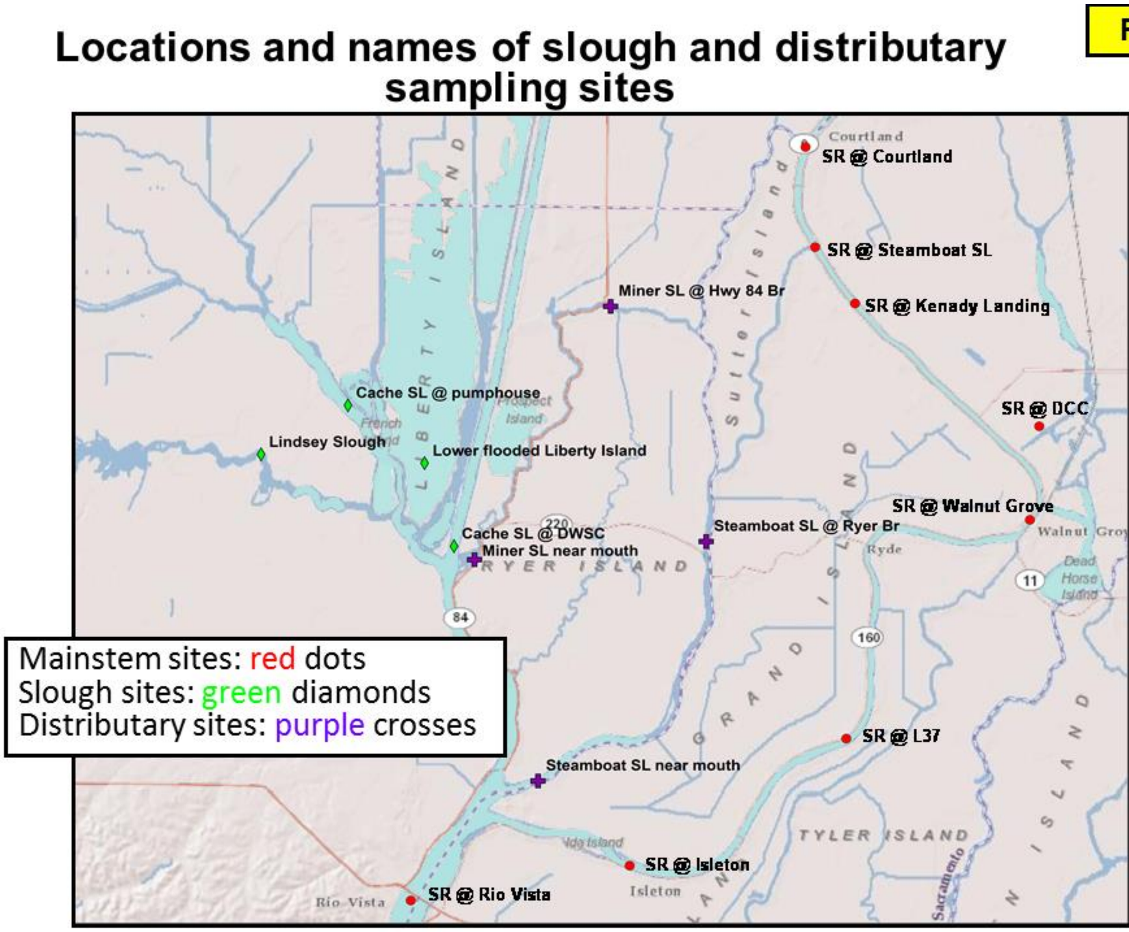

Figure 4

This map is an expanded version of **Figure 2** that includes the site names for sampling sites on **sloughs** in the Cache/Yolo Complex and **distributaries** on Miner and Steamboat Sloughs – and at some upper Sacramento River **mainstem** locations; see Table 1 for more information about the sites.

Fig. 5

Locations and names of Delta and Bay sampling sites

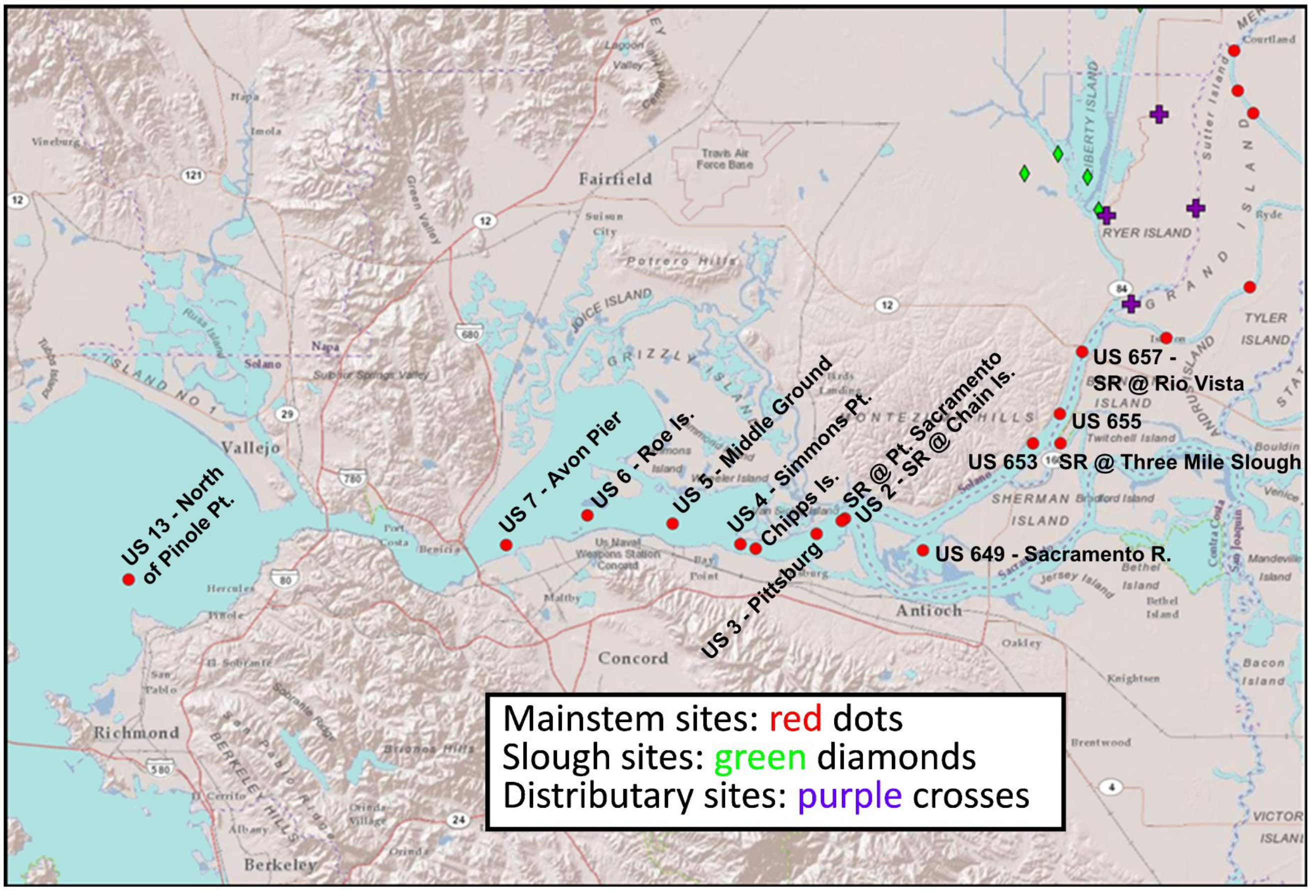

Figure 5
This map is an expanded version of **Figure 2** that includes the site names for **mainstem** Sacramento River sampling sites in the Delta and Northern San Francisco Bay; see Table 1 for more information about the sites.

Fig. 6

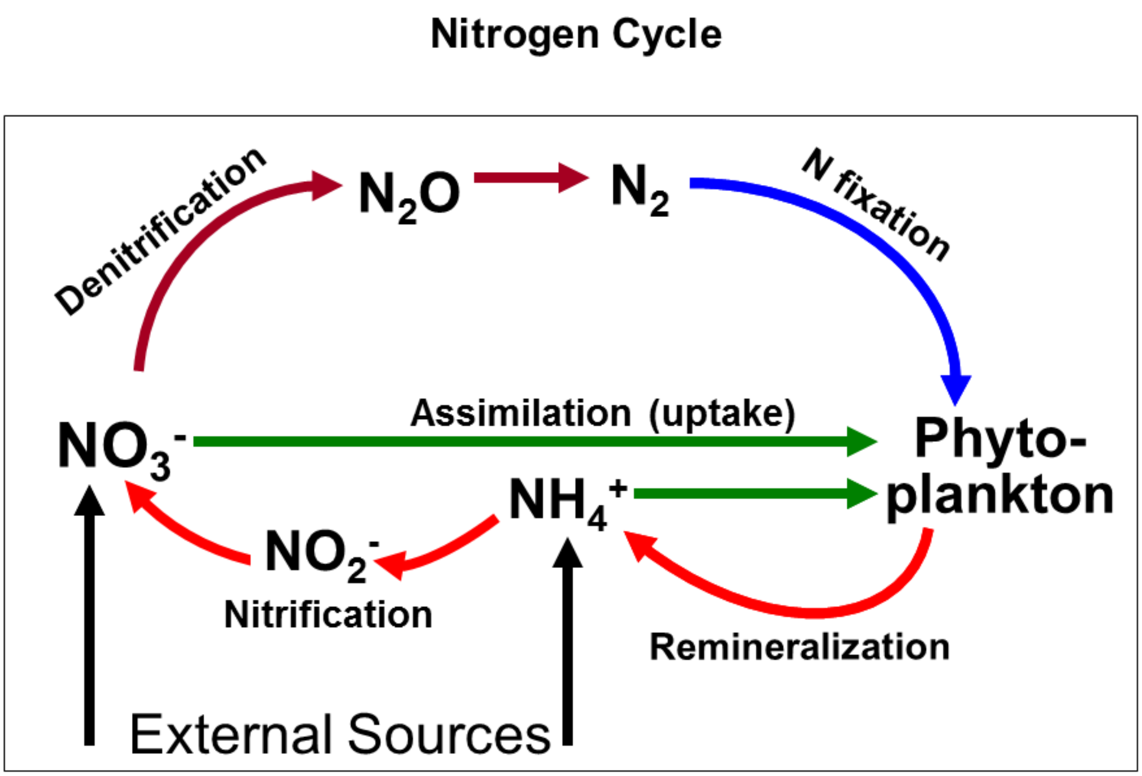

Figure 6
This cartoon shows the main sources of N to a typical aquatic ecosystem and the main biogeochemical processes that convert one form of N to another. Note that phytoplankton (as well as cyanobacteria) can derive N from 3 different sources: N fixation, NH_4 assimilation, and NO_3 assimilation. The main external sources of NH_4 are waste water treatment plant effluent, animal manure, and fertilizer. The main external sources of NO_3 are fertilizer and nitrification of NH_4 from waste water treatment plant effluent, animal manure, and fertilizer.

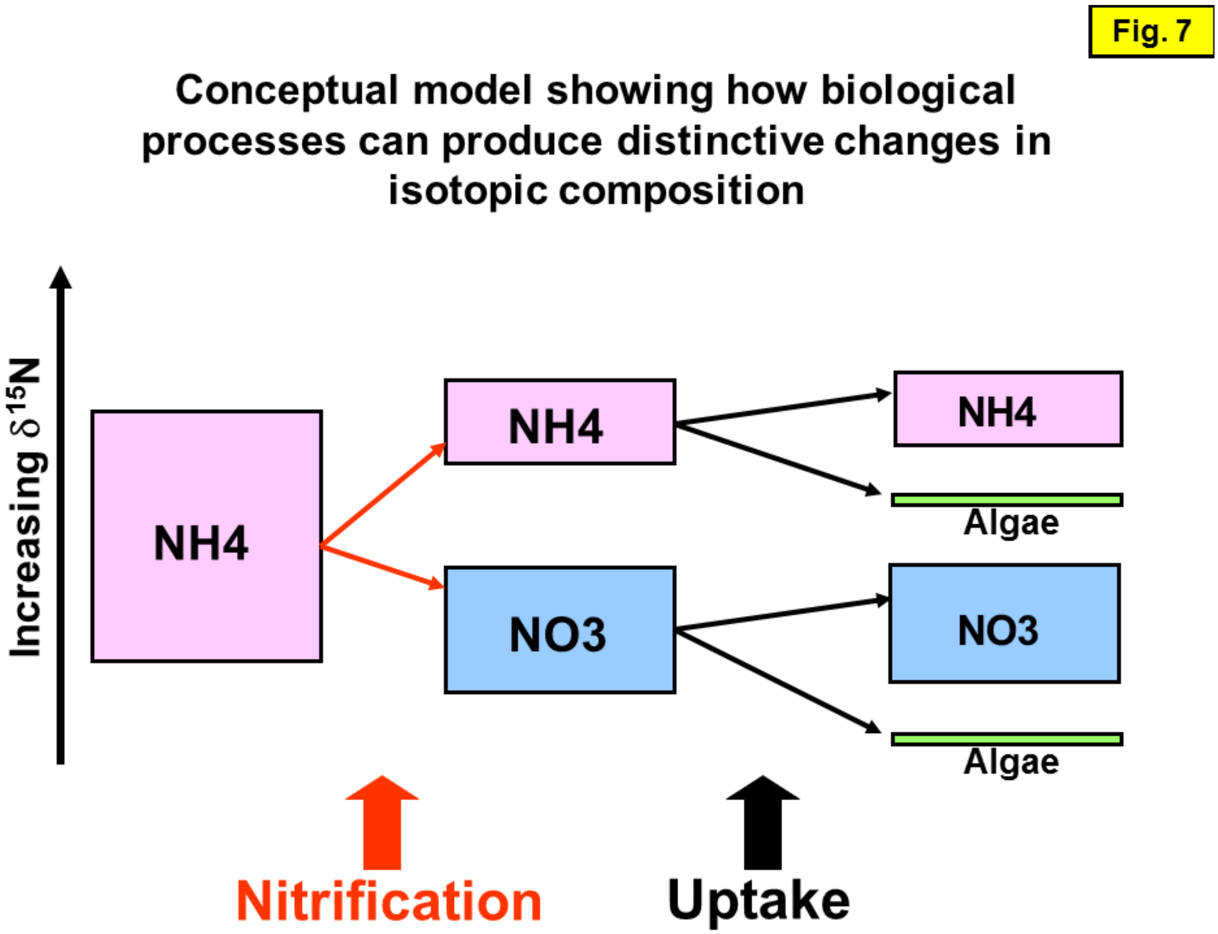

Figure 7

This cartoon shows how nitrification and uptake can cause shifts in the $\delta^{15}N$ of the resulting NH_4, NO_3, and algae pools. The sizes of the boxes APPROXIMATE the relative amounts of N in algae and nutrients during NH_4 and NO_3 uptake, and the relative vertical positions of the boxes APPROXIMATE their relative $\delta^{15}N$ values. These boxes are not to scale in that the uptake rate of NH_4 is about an order of magnitude higher than that of NO_3 (Parker et al., 2012). The main principle is that biogeochemical processes preferentially utilize more of the lower-mass isotopes (e.g., ^{14}N instead of ^{15}N), causing “isotope fractionations” that result in new products to have lower $\delta^{15}N$ values than the starting compositions, and residual substrates having higher $\delta^{15}N$ values.

Fig. 8

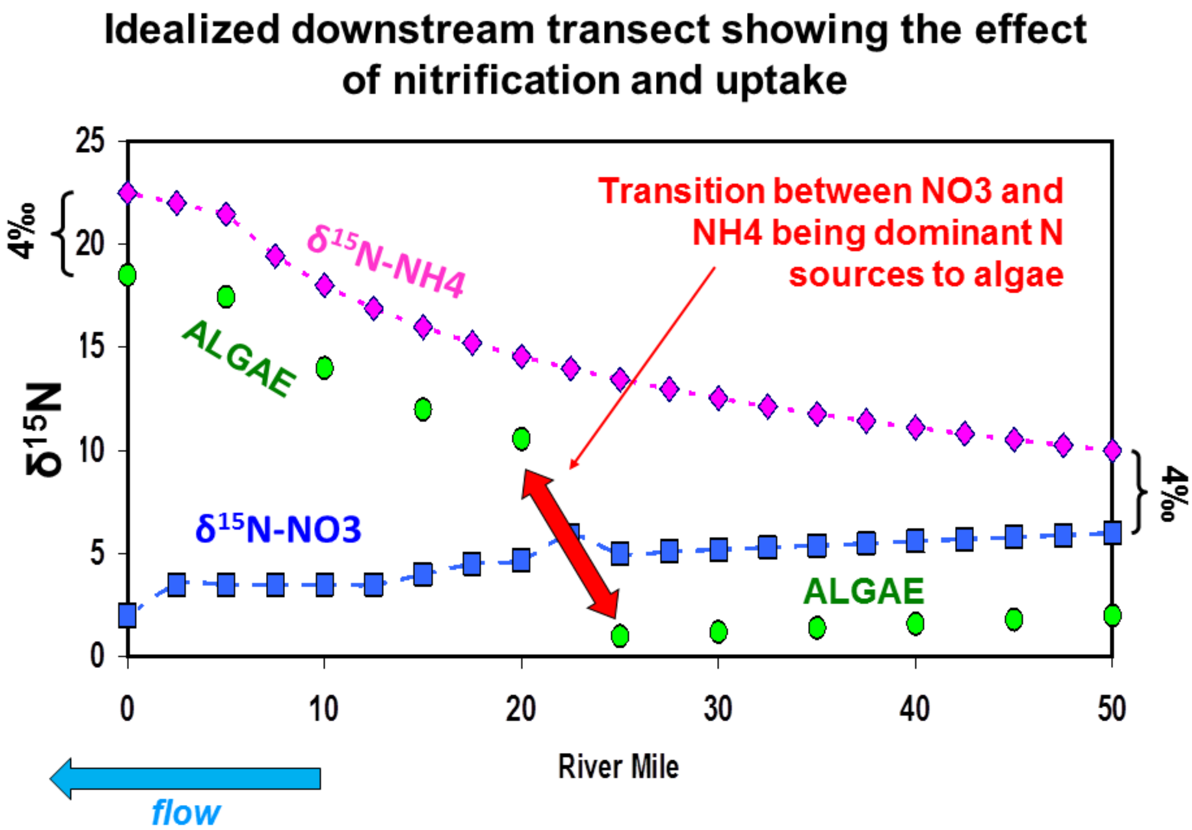

Figure 8

This cartoon illustrates the idealized trends in $\delta^{15}N$ for NH_4, NO_3 and algae during progressive downstream nitrification. Since algae and bacteria will utilize the lower-mass isotopic fraction first, the $\delta^{15}N$ of the algae will be lower than the $\delta^{15}N$ of the N being assimilated; this cartoon uses a 4‰ fractionation for both NO_3 and NH_4 assimilation. At upstream sites, the $\delta^{15}N$ of algae is 4‰ lower than the $\delta^{15}N$-NO_3, which is consistent with algae mainly assimilating NO_3. However, downstream of RM25, the $\delta^{15}N$ of algae becomes higher than the $\delta^{15}N$-NO_3, which means that the NO_3 cannot be a significant source of N to algae at these sites. Hence, there is a transition at RM25 from algae assimilating NO_3 to algae assimilating NH_4, in this case again with a 4‰ fractionation.

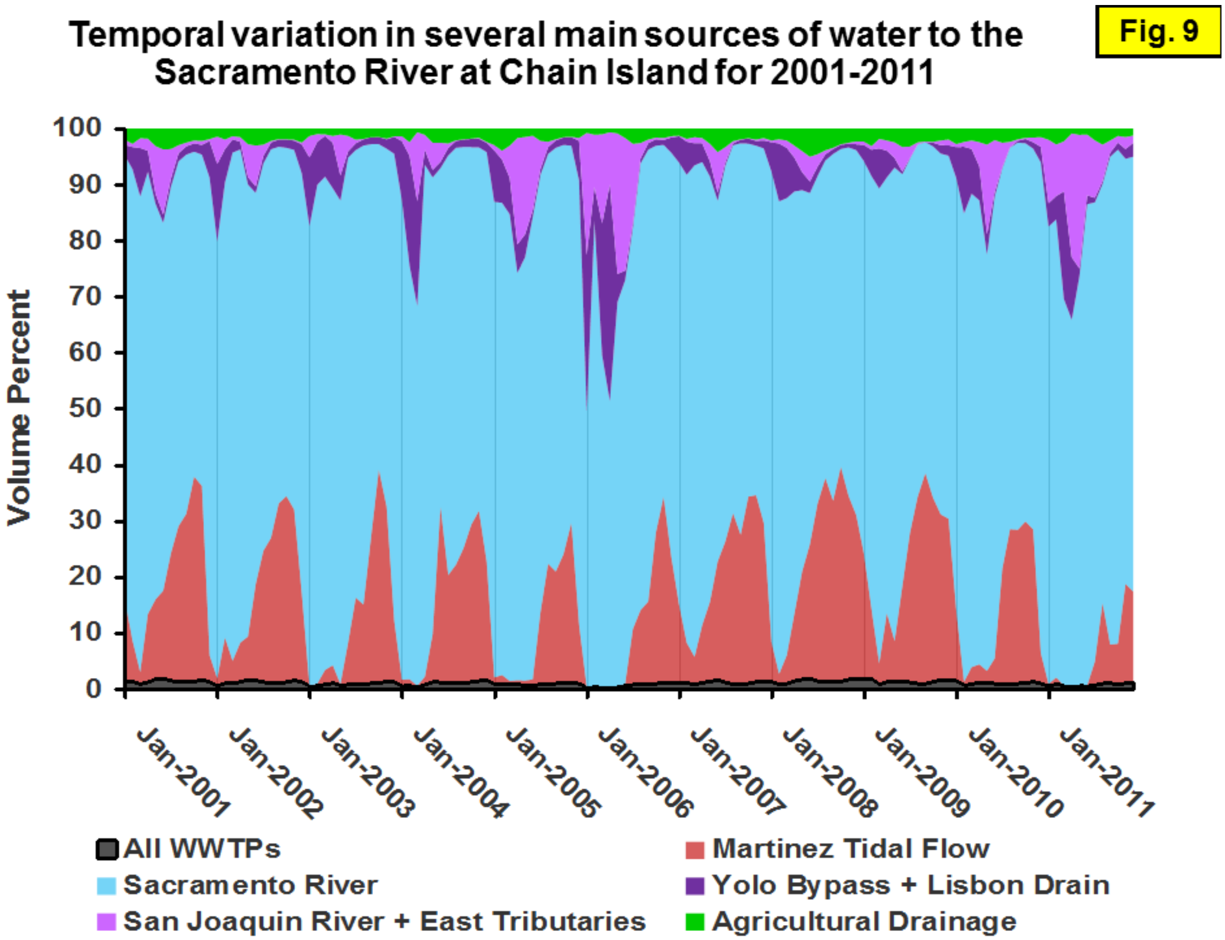

Figure 9

Seasonal variations in the relative contributions of different sources of water to the Sacramento River at Chain Island for the years 2001-2011. The Chain Island site on the Sacramento River is located at the confluence with the San Joaquin River at River Mile = 0 (denoted RM0). These estimates were made using the Delta Simulation Model II (DSM2), a one-dimensional mathematical model for dynamic simulation of one-dimensional hydrodynamics, water quality, and particle tracking in a network of riverine or estuarine channels. Determination of the sources of nutrients to specific locations is complicated by the considerable seasonal variation in the major sources of water to these locations.

Fig. 10

Temporal variation in stage is mostly caused by tidal cycles

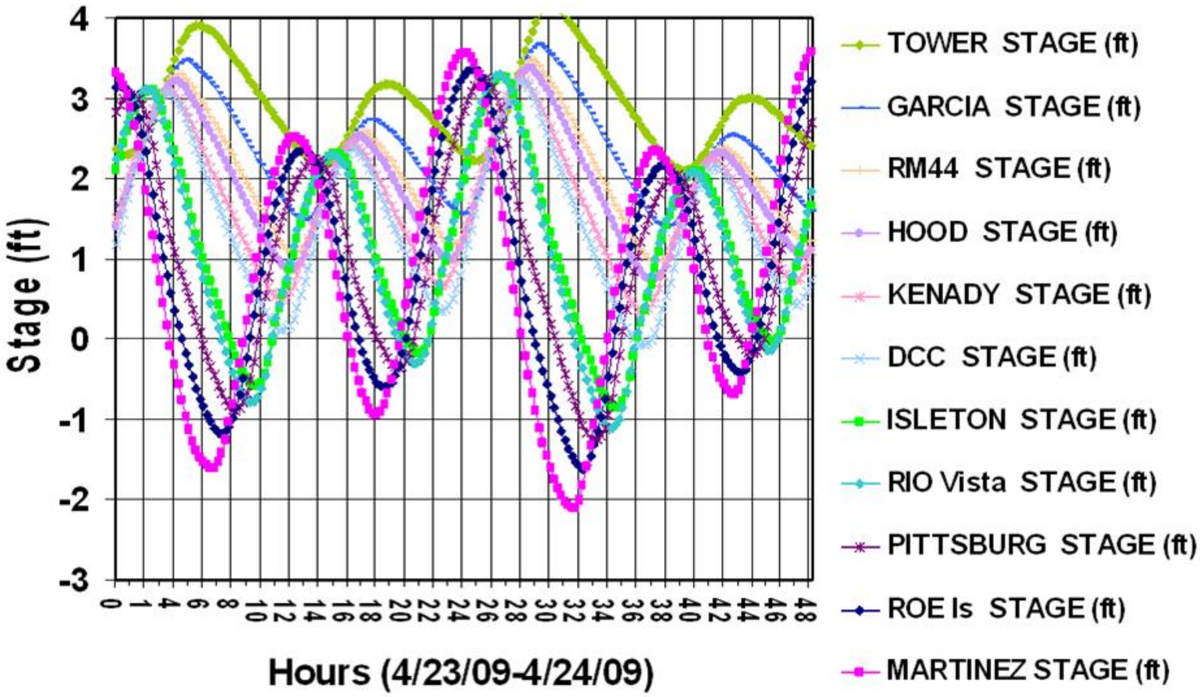

Figure 10

Temporal variations in river stage (water level height, in feet) over 48 hours for 11 sites on the Sacramento River, from Tower Bridge (RM59) to Martinez (RM-17). Most of the locations with stage data are sites where samples were collected (see Table 1). These temporal variations are caused by the semi-diurnal tidal cycle in the ocean, with two high water-levels (of different heights) and two low-water levels (of different heights) each day. The amplitudes of the tidal cycles increase downstream. The tide reverses direction every 8-14 hours, making it difficult to collect all the samples on the ebb tide.

Fig. 11

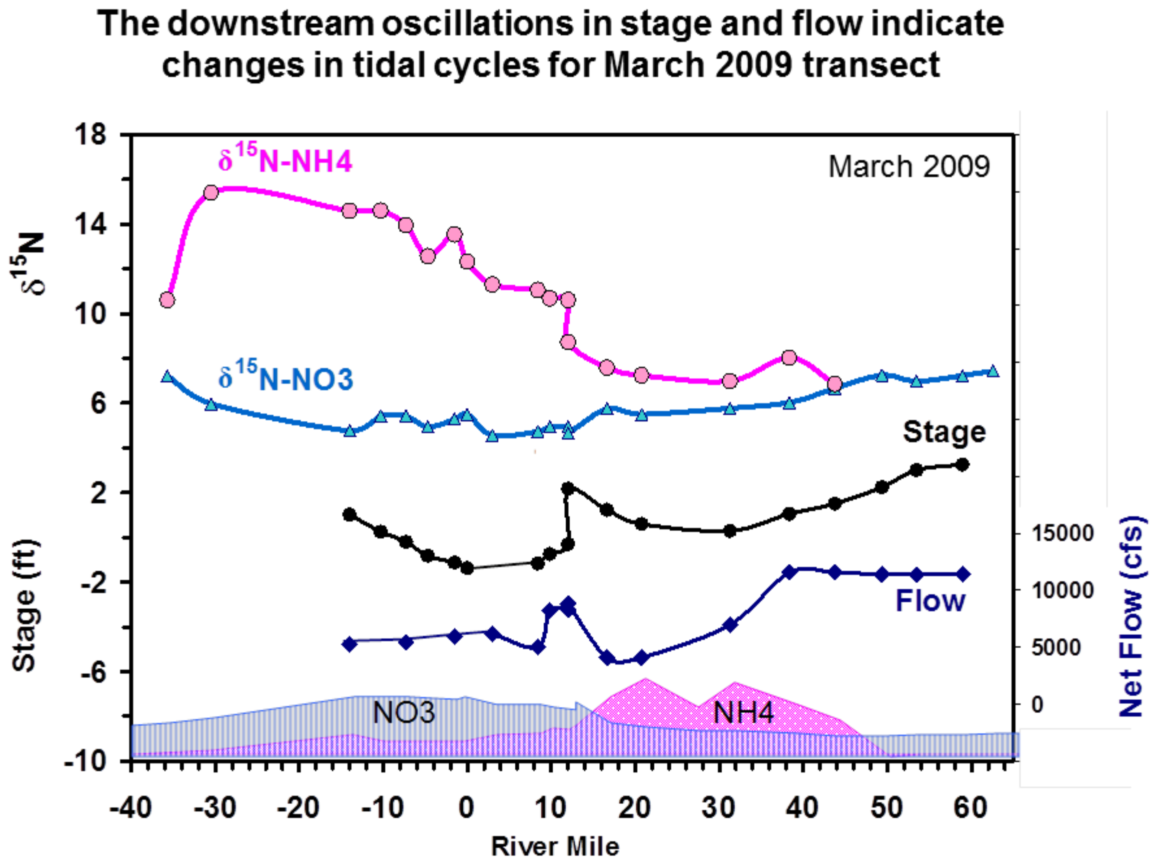

Figure 11

Downstream variation in the $\delta^{15}N$ values of NH_4 and NO_3, and in stage and net flow for the March 2009 transect are plotted as symbols and lines; the corresponding NH_4 and NO_3 concentrations (sometimes denoted as $[NH_4]$ and $[NO_3]$, respectively), are plotted as overlapping color blocks at the bottom of the plots. The net (not instantaneous) flow data are from the DSM2 model. Increases in $[NO_3]$ and decreases in $[NH_4]$ downstream from this point result from nitrification of effluent-derived NH_4. Downstream changes in stage and net (not instantaneous) flow are also shown (net flow data from the DSM2 model). Samples were collected over 4 consecutive tidal cycles, sampling from upstream to downstream. The downstream oscillations in stage and flow reflect changes in tidal cycles during the two days of sampling (March 26th and 27th). The drop in net flow at ~RM38 reflects diversion of ~50% of the flow of the Sacramento River to Miner and Steamboat Sloughs.

Fig. 12

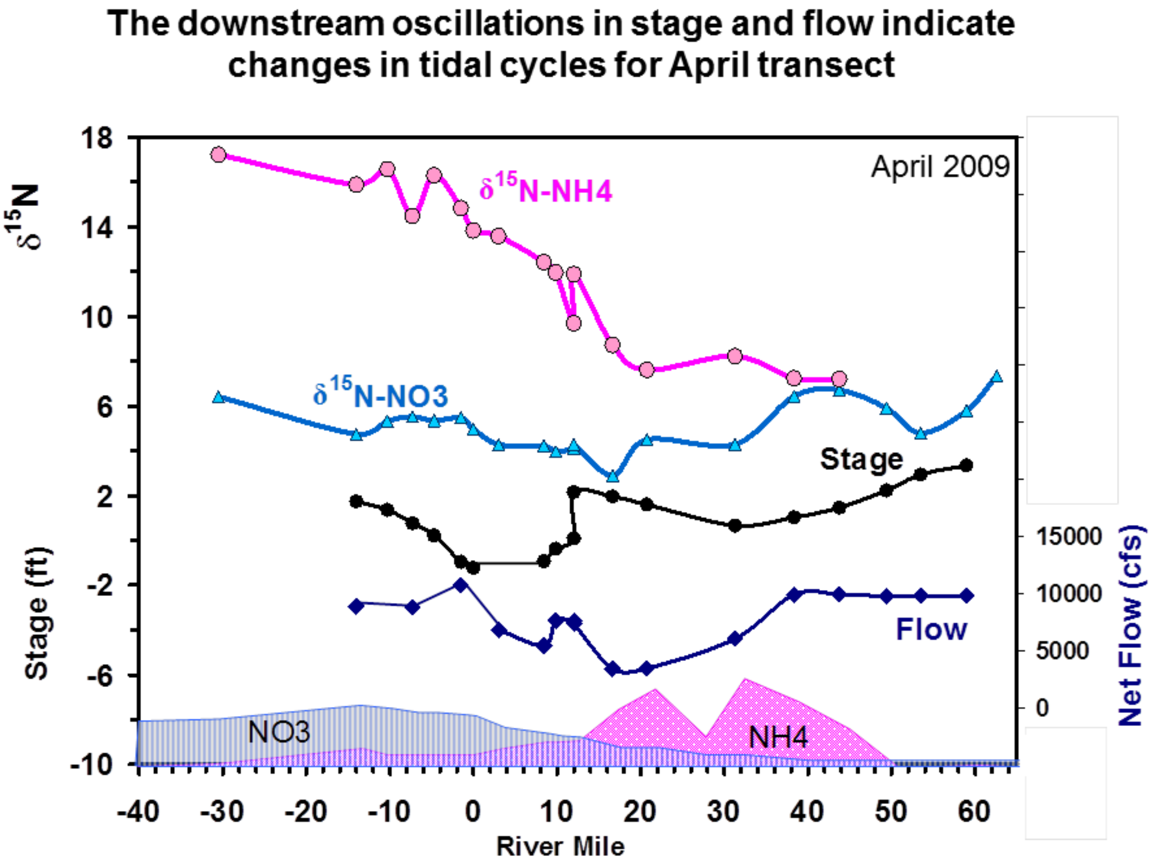

Figure 12

Downstream variation in the $\delta^{15}N$ values of NH_4 and NO_3, and in stage and net flow for the April 2009 transect are plotted as symbols and lines; the corresponding NH_4 and NO_3 concentrations (sometimes denoted as [NH_4] and [NO_3], respectively), are plotted as overlapping color blocks at the bottom of the plots. The net (not instantaneous) flow data are from the DSM2 model. The Sacramento Regional Water Treatment Plant (SRWTP) releases treated wastewater effluent to the river at ~RM46. Increases in [NO_3] and decreases in [NH_4] downstream from this point result from nitrification of effluent-derived NH_4. Downstream changes in stage and net (not instantaneous) flow are also shown (net flow data from the DSM2 model). Samples were collected over 4 consecutive tidal cycles, sampling from upstream to downstream. The downstream oscillations in stage and flow reflect changes in tidal cycles during the two days of sampling (April 23rd and 24th). The drop in net flow at ~RM38 reflects diversion of ~50% of the flow of the Sacramento River to Miner and Steamboat Sloughs.

Fig. 13

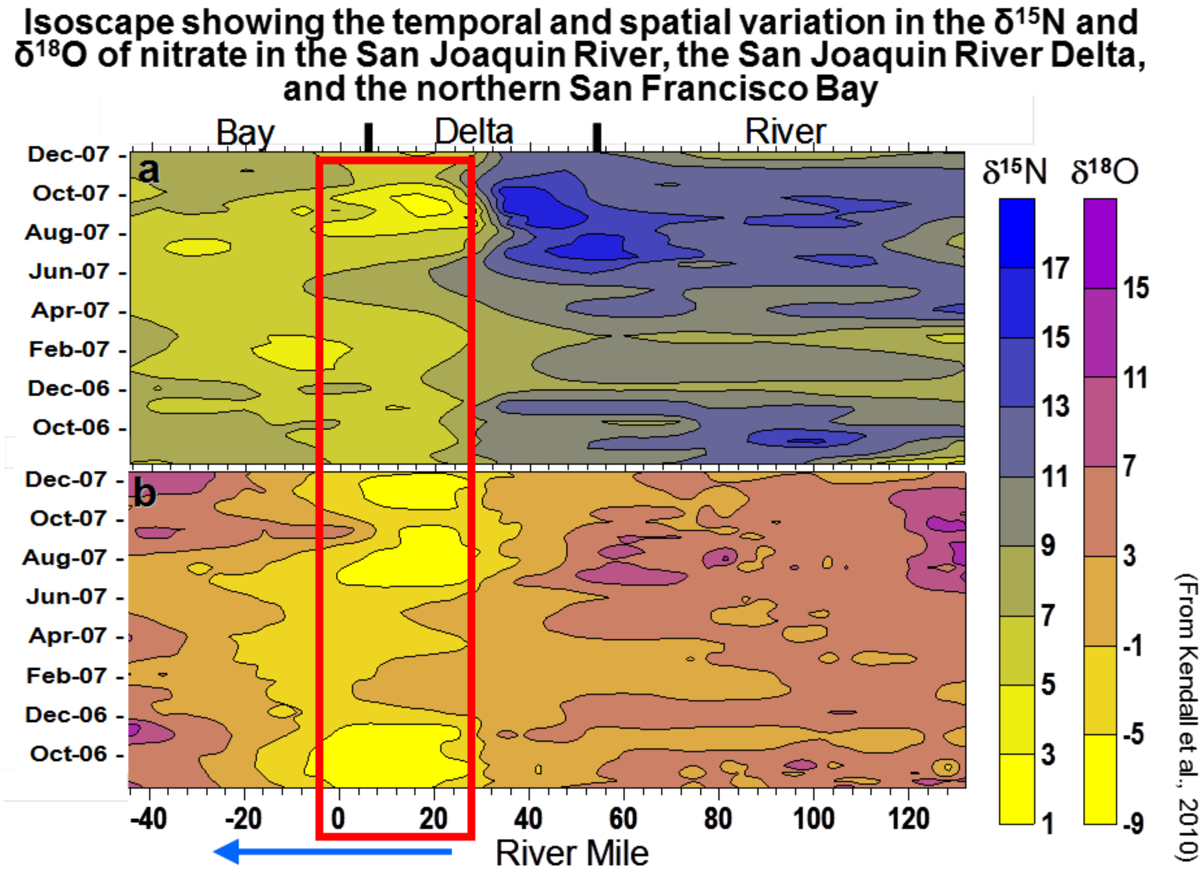

Figure 13

Spatial and temporal distribution of nitrate-$\delta^{15}N$ values (a) and nitrate-$\delta^{18}O$ values (b) along 170 miles of river, extending from the headwaters of the San Joaquin River, through areas receiving Central Valley agricultural return waters through the Sacramento-San Joaquin Delta, and across the northern San Francisco Bay to where the estuary drains into the Pacific Ocean (see map, Figure 14). River miles are measured from where the San Joaquin River converges with the larger Sacramento River (RM0), with positive values representing upstream locations and negative values representing downstream locations. This plot reflects data from ~1200 samples collected August 2006-December 2007. The red-bordered box extending from ~RM-4 to RM28 encloses a section of the transect with $\delta^{15}N$ and $\delta^{18}O$ values of nitrate that are significantly lower than locations upstream and downstream of this section. Figure modified from Kendall et al. (2010).

Fig. 14

Map of San Francisco Estuary sites sampled 2005-2007

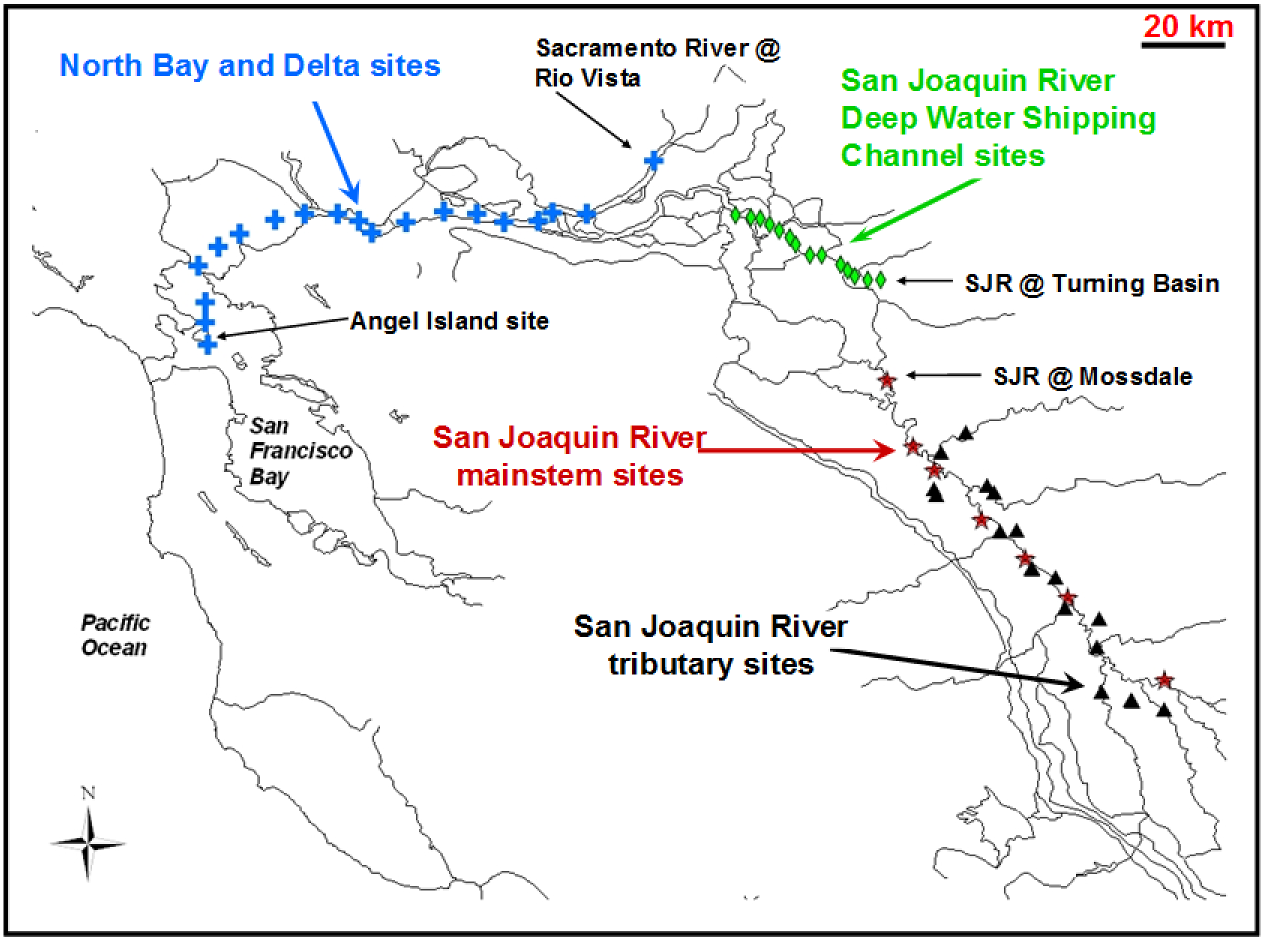

Figure 14

This map shows the locations of sites sampled as part of several studies 2005-2007. Only isotope data from the mainstem (main channel) sites were used to prepare **Figure 13** (Kendall et al., 2010). The mainstem samples include sites on the main channel of the San Joaquin River (RM109 to RM56; note different symbols for different San Joaquin River site types), on the main channel of the upper (deltaic) San Joaquin River (RM41 to RM24), and then on the main channel of the lower (deltaic) Sacramento River (RM12 to RM-45). The San Joaquin River converges with the Sacramento River at RM0.

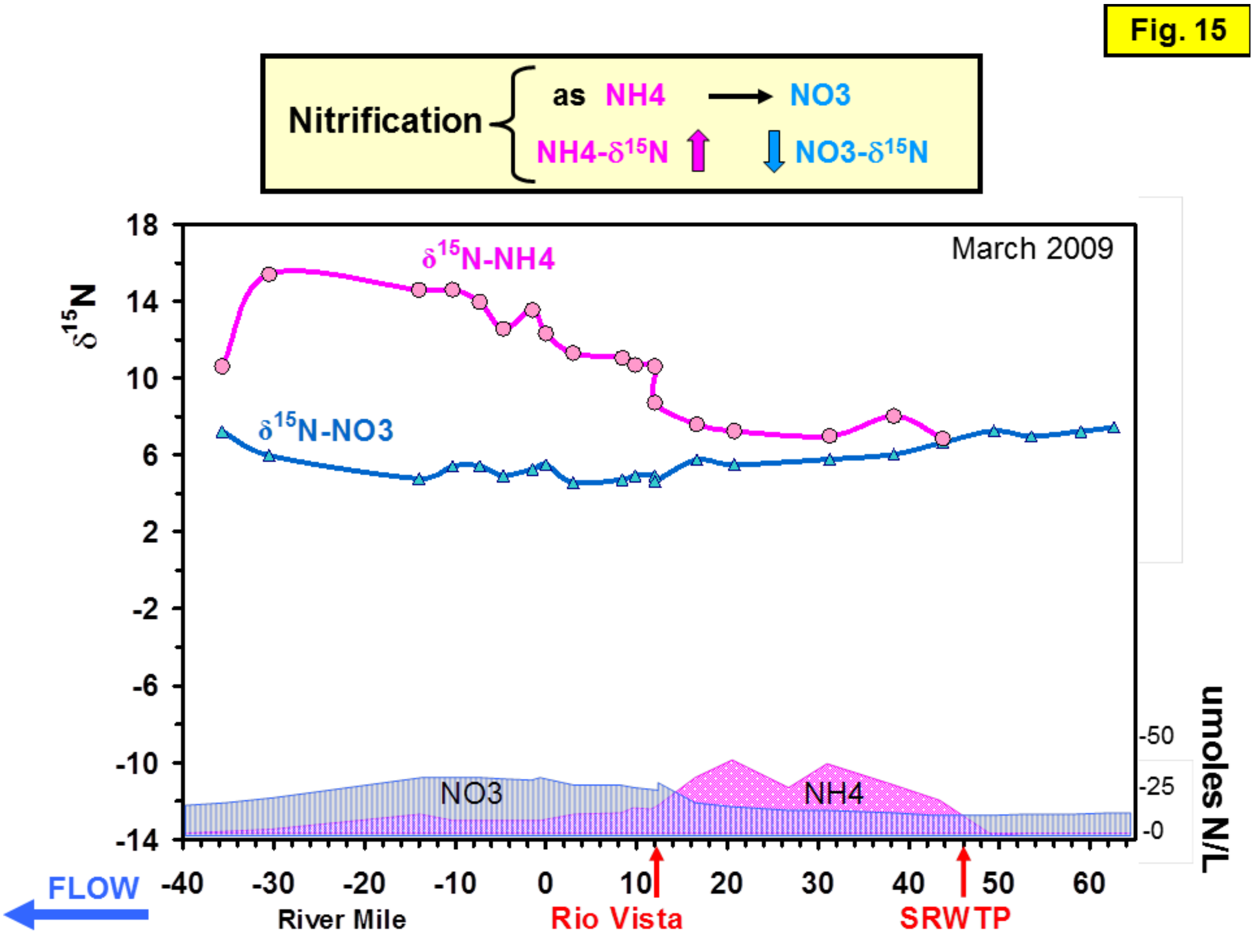

Figure 15

Downstream variation in the $\delta^{15}N$ values and concentrations of NH_4 and NO_3 for the March 2009 transect of the Sacramento River. The schematic at the top illustrates the relationships among the parameters: as a fraction of the NH_4 pool (a fraction with lower $\delta^{15}N$) undergoes nitrification, the newly formed NO_3 has a lower $\delta^{15}N$ than the original NH_4, causing the $\delta^{15}N$ of the remaining pool of NH_4 to increase. This downstream increase in the $\delta^{15}N$-NH_4 is gradual while NH_4 concentrations are high, and then increased rapidly as NH_4 concentrations drop downstream. The spatial variations of these data, especially the $\delta^{15}N$-NH_4 values, clearly show the effect of gradual nitrification of NH_4 to NO_3. All data for the Delta Cross Channel (DCC) site at RM27 are omitted. SRWTP: indicates where treated effluent from the Sacramento Regional Wastewater Treatment Plant enters the River.

Fig. 16

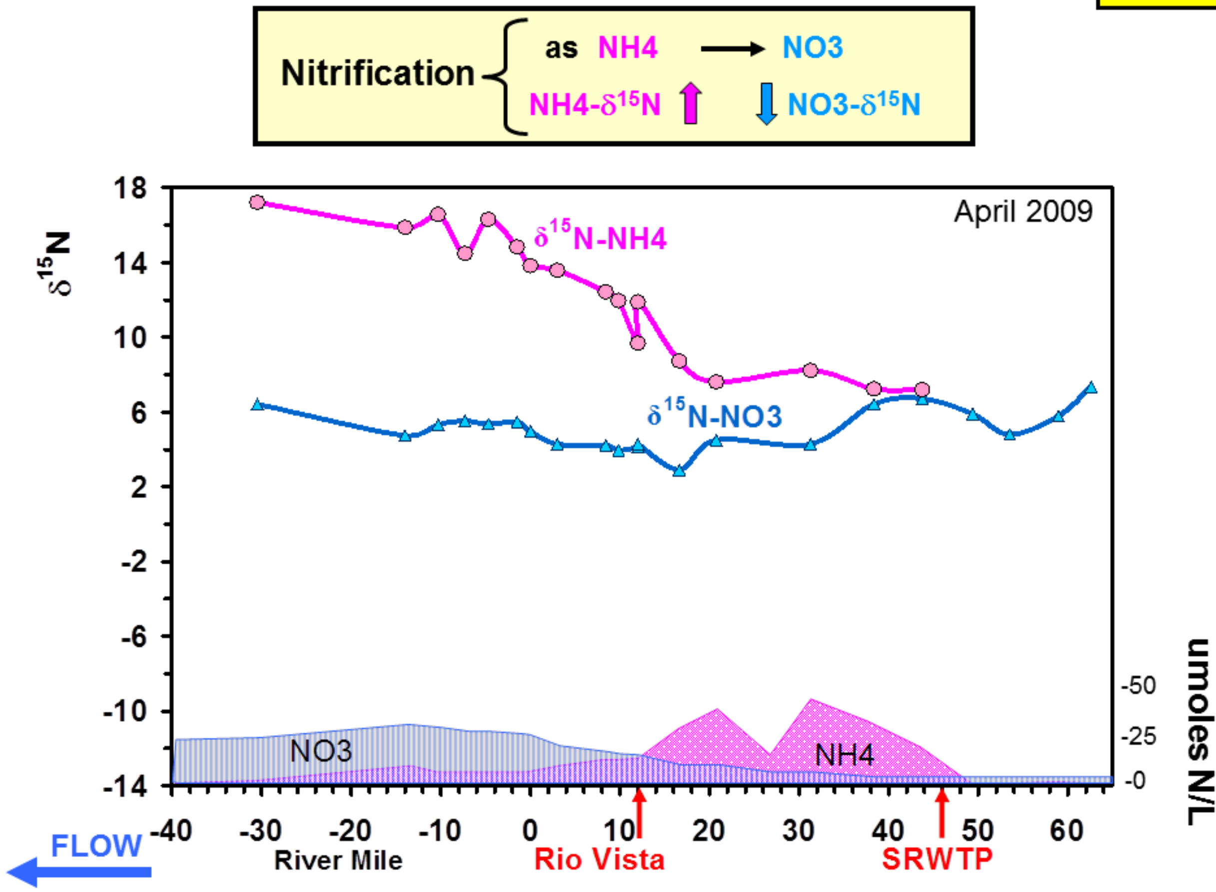

Figure 16

Downstream variation in the $\delta^{15}N$ values and concentrations of NH_4 and NO_3 for the April 2009 transect of the Sacramento River. The schematic at the top illustrates the relationships among the parameters: as a fraction of the NH_4 pool (a fraction with lower $\delta^{15}N$) undergoes nitrification, the newly formed NO_3 has a lower $\delta^{15}N$ than the original NH_4, causing the $\delta^{15}N$ of the remaining pool of NH_4 to increase. This downstream increase in the $\delta^{15}N$-NH_4 is gradual while NH_4 concentrations are high, and then increased rapidly as NH_4 concentrations drop downstream. The spatial variations of these data, especially the $\delta^{15}N$-NH_4 values, clearly show the effect of gradual nitrification of NH_4 to NO_3. All data for the Delta Cross Channel (DCC) site at RM27 are omitted. SRWTP: indicates where treated effluent from the Sacramento Regional Wastewater Treatment Plant enters the River.

Fig. 17

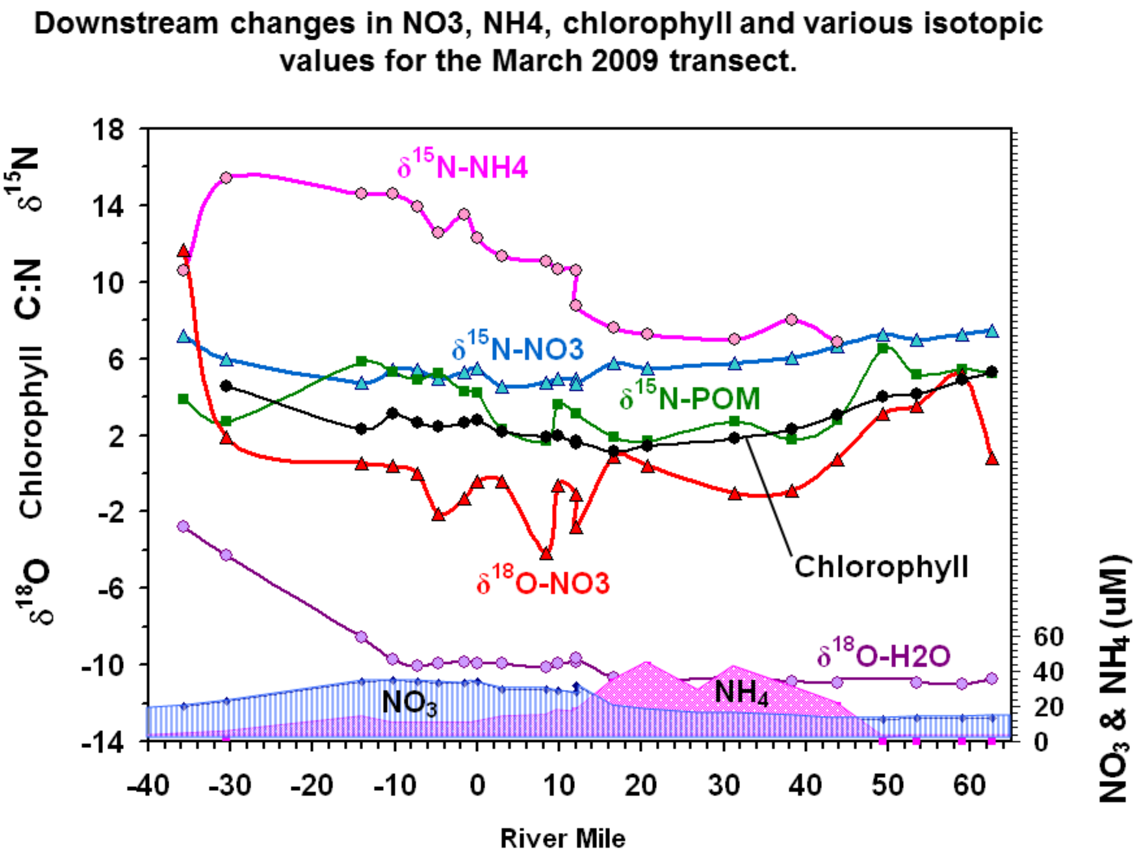

Figure 17

Downstream variation in the $\delta^{15}N$ values of NO_3, NH_4, and POM; the $\delta^{18}O$ of NO_3 and H_2O; and chlorophyll-a concentration for March 2009 transect of the Sacramento River. The isotope and chlorophyll data for the Delta Cross Channel (DCC) site at RM27 are omitted.

Fig. 18

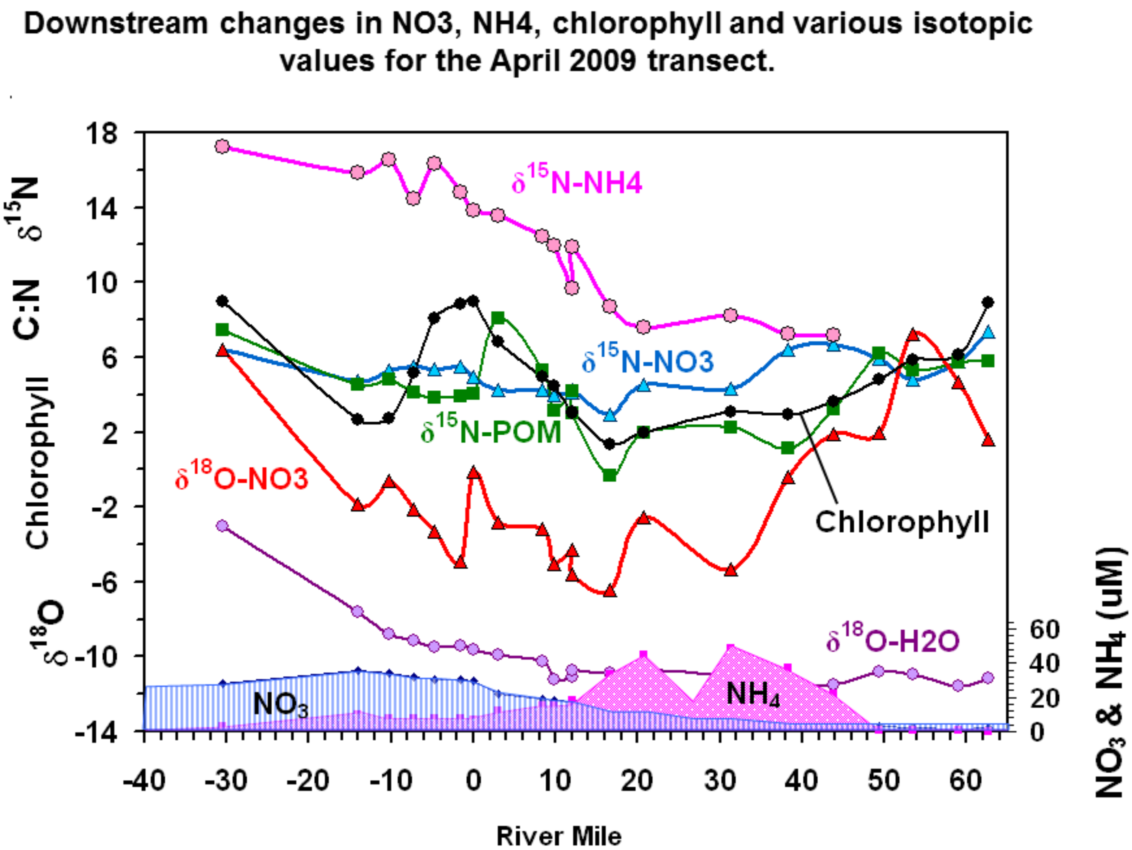

Figure 18

Downstream variation in the $\delta^{15}N$ values of NO_3, NH_4, and POM; the $\delta^{18}O$ of NO_3 and H_2O; and chlorophyll-a concentration for the April 2009 transect of the Sacramento River. The isotope and chlorophyll data for the Delta Cross Channel (DCC) site at RM27 are omitted. Note the algal bloom at the confluence of the SJR (RM0), shown by the increase in chlorophyll. The “spike” in the $\delta^{15}N$ of the POM upstream of RM0 may reflect tidal sloshing of algae derived from the confluence area. The progressive increase in the $\delta^{18}O$ of H_2O downstream of RM12 and especially downstream of RM-10 reflects mixing with marine water of ~ $\delta^{18}O\text{-}H_2O = 0$.

Fig. 19

The mirror images of the lines show the effects of nitrification

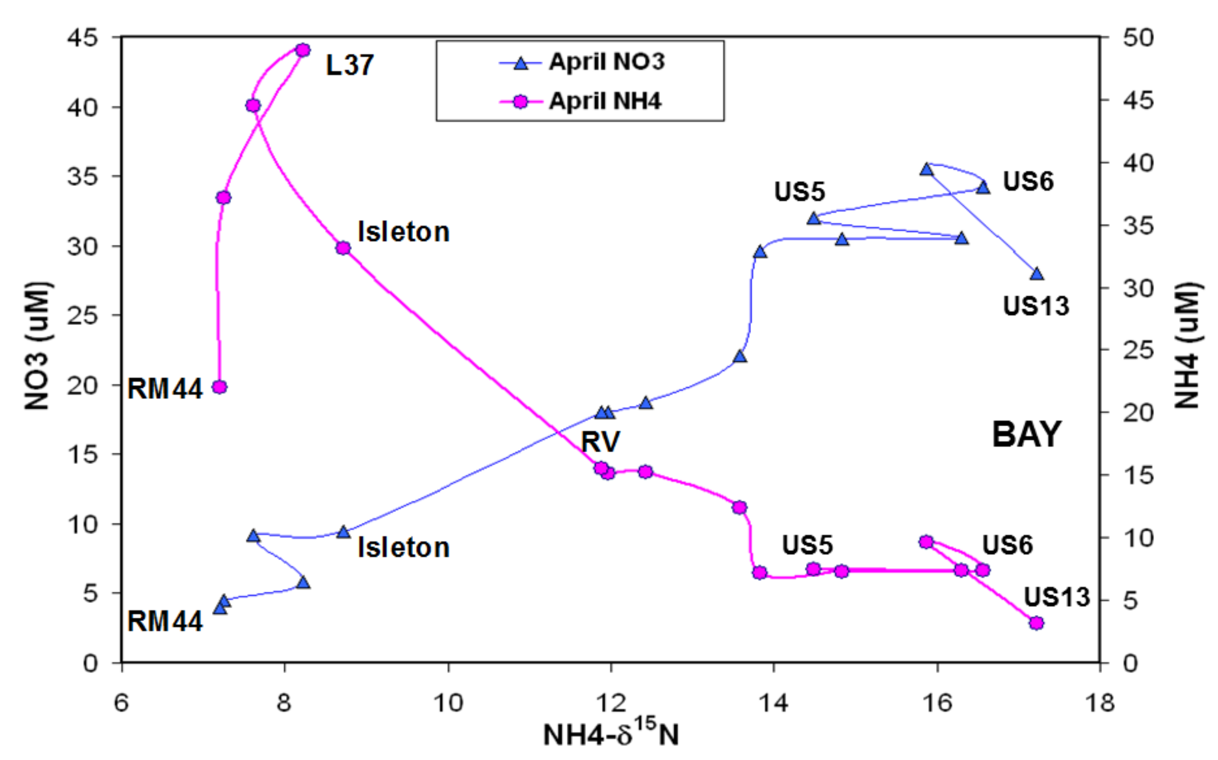

Figure 19

The downstream changes in NH_4 and NO_3 concentration for samples collected during the April 2009 transect of the Sacramento River from RM44 to the Bay (site US13) are plotted relative to $\delta^{15}N$ of NH_4 to show the effects of nitrification (conversion of NH_4 to NO_3) on nutrient concentrations and NH_4-$\delta^{15}N$. No data are presented for sites upstream of RM44 because the NH_4 concentrations were too low above the entry point of wastewater effluent for analysis of $\delta^{15}N$-NH_4; data from the DCC site were omitted. The NO_3 and NH_4 lines are approximately mirror images of each other for the section of the transect with for NH_4-$\delta^{15}N$ values ranging from about +8 to +16‰, consistent with nitrification being the dominant biogeochemical process acting on these two pools of N in this section of the river. The oscillations in NH_4 and NO_3 concentration between the RM44 site and Isleton are likely due to variability in wastewater effluent input, as well as tidal reversals which affect the amount of NH_4 that has been converted to NO_3 via nitrification (O'Donnell 2014). The reversal between the US5 (Middle Ground, RM-7) and the US13 (North of Pinole Point, RM-30) reflects a local source of NH_4 (Figure 18). However, this section of the transect also shows the downstream transition from the tidally dominated river channel to the more open Bay, where mixing with marine water becomes the dominant process affecting water chemistry and isotopes. This transition to a mixing zone is best illustrated by the dramatic changes in water-$\delta^{18}O$ values downstream of about RM-10 (**Figure 18**).

Fig. 20

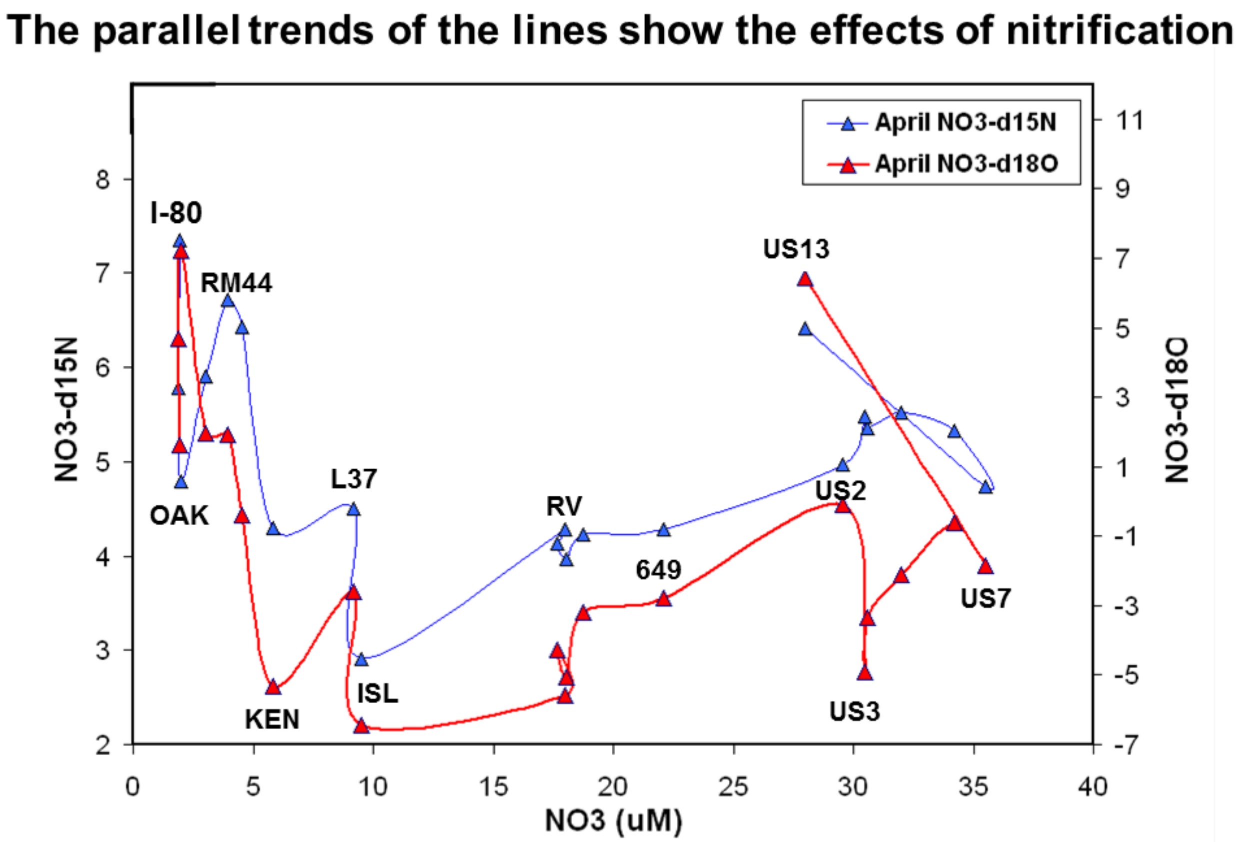

Figure 20

The downstream changes in NO_3-$\delta^{15}N$ and NO_3-$\delta^{18}O$ for samples collected during the April 2009 transect of the Sacramento River from the I-80 Bridge (RM63)to the Bay (site US13, RM-31) are plotted relative to NO_3 concentrations. The matching trends of the two lines show that the $\delta^{15}N$ and $\delta^{18}O$ values are closely "coupled", which is consistent with nitrification being the dominant process affecting NO_3 isotopic compositions in the Sacramento River downstream of the WWTP (Figure 18); however, mixing of riverine and Bay (marine) sources of nitrate downstream of about RM-10 (Figure 18) could also account for the trends in this section of the transect. The "out of phase" trends upstream of RM44 reflect the upstream origin of the NO_3 upstream of SRWTP.

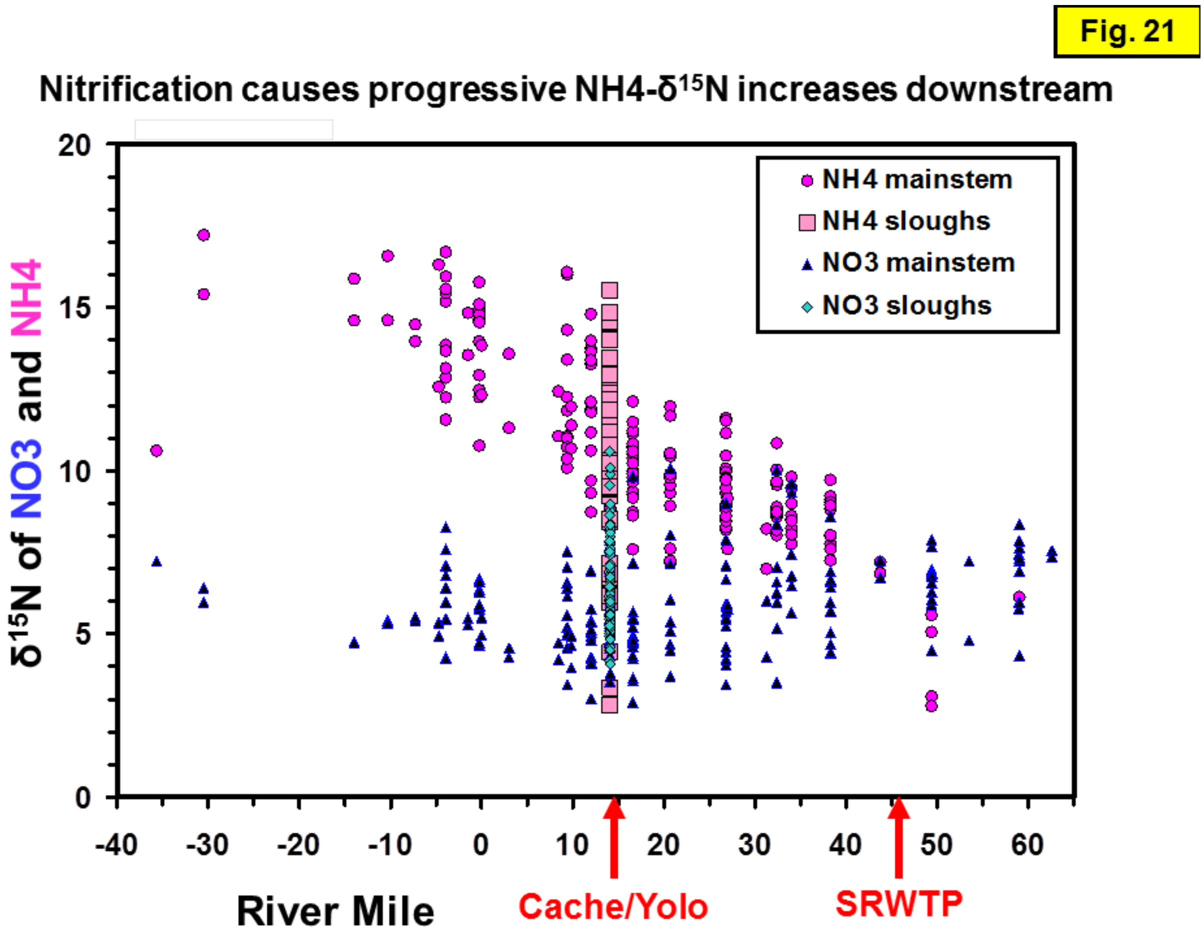

Figure 21

Comparison of $\delta^{15}N$ values of NO_3 (pink/violet) and NH_4 (blue/aqua) plotted against River Mile for samples collected at mainstem and slough locations of the Sacramento River for all transects. Symbol shape identifies mainstem versus slough locations. The entry points of SRWTP effluent and water from the Cache/Yolo Complex sloughs are shown with red arrows. All the slough samples are plotted at RM14.1 because the various sloughs sampled all drain into Cache Slough and this RM value is where Cache Slough converges with the mainstem Sacramento River. The data show the overall downstream trend of increasing NH_4-$\delta^{15}N$ as an isotopically light fraction of the ammonium pool is preferentially converted to nitrate (nitrification).

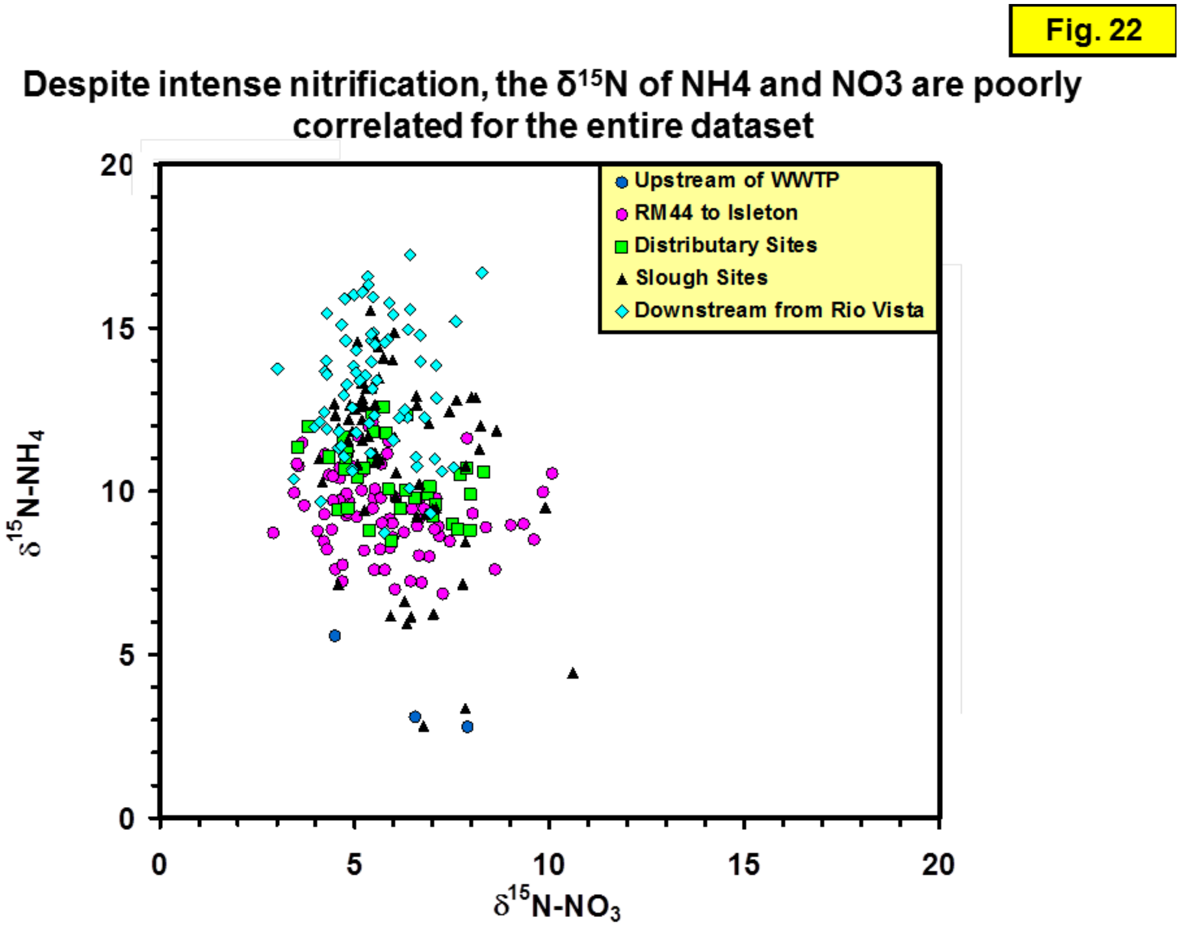

Figure 22
Comparison of the $\delta^{15}N$ values of NO_3 and NH_4 for all sites sampled on all Sacramento River transects. Different symbol shapes and colors indicate sample types (e.g., distributary and slough sites) and section of the river for mainstem sites.

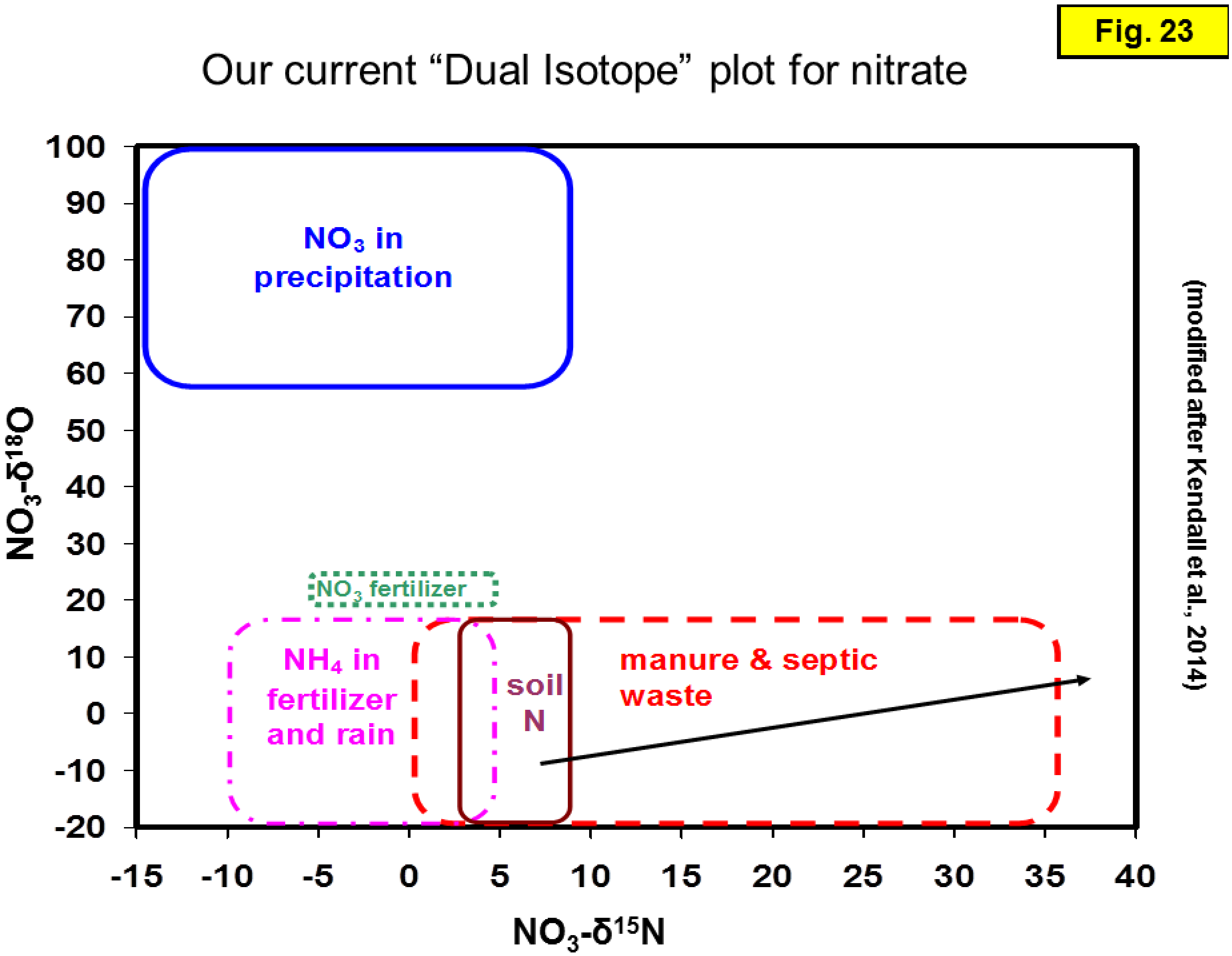

Figure 23

This plot shows a revised version of the original Kendall (1998) plot that summarized the dominant compositional ranges of all available $\delta^{15}N$ and $\delta^{18}O$ data for nitrate; the compositional boxes have been adjusted for additional data. The black arrow shows a typical slope for a groundwater denitrification line, with a slope of 2:1. Slopes as low as 1:1 are not uncommon in lab studies (and some field studies). The ranges in the $\delta^{18}O$ values reflect the ranges in the ambient $\delta^{18}O$ of water and O_2 gas during nitrification (Kendall et al., 2007).

Fig. 24

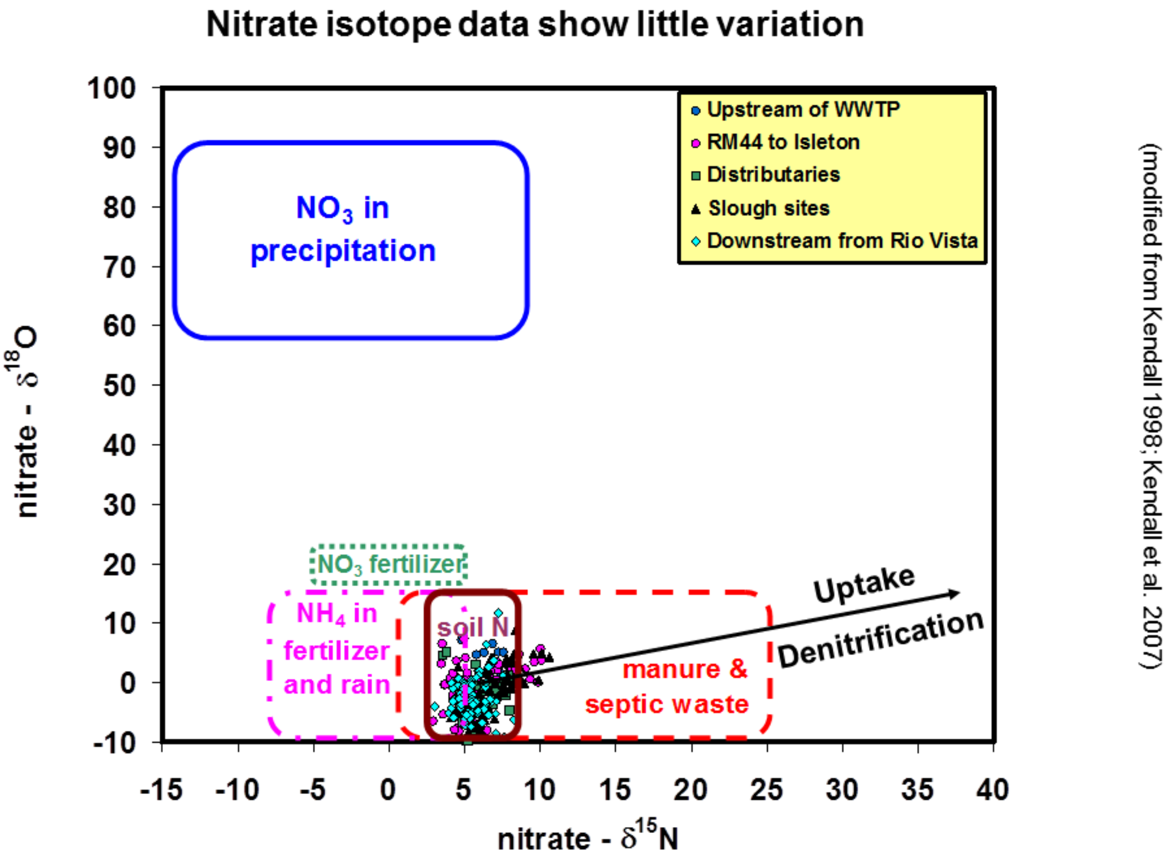

Figure 24
Nitrate $\delta^{15}N$ and $\delta^{18}O$ values for all sites and dates are plotted on a dual isotope plot (Kendall et al., 2007). Samples from different types and locations of sites are denoted by different symbol colors and shapes. The expected trend for uptake (and denitrification) is shown as a thin black arrow. Despite all the N-cycling in the ecosystem, the isotopic compositions of NO_3 have not changed very much from what would be considered "typical" NO_3 derived from a mixture of soil, agricultural, and septic waste sources. See **Figure 25** for details.

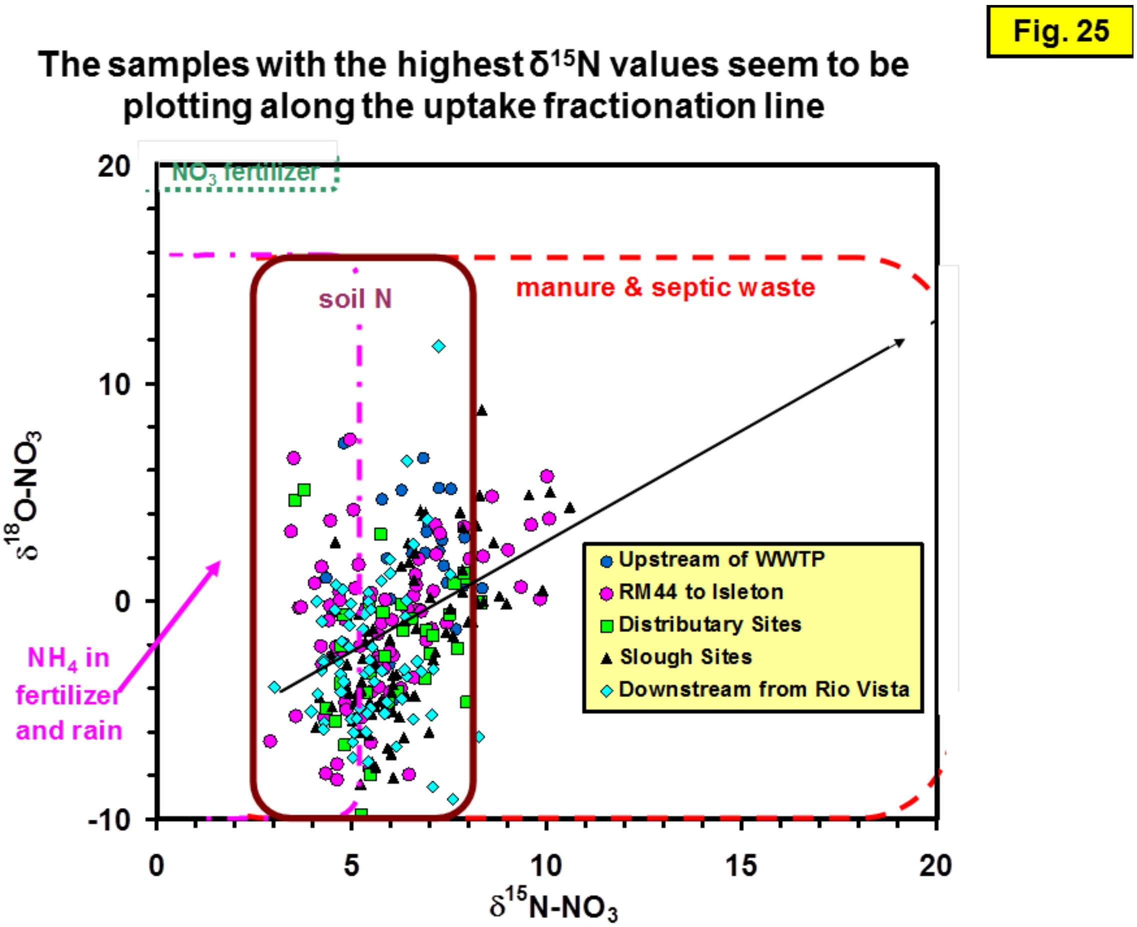

Figure 25

This plot expands the scale of the previous plot (**Figure 24**) to show that samples collected upstream of the WWTP tend to have slightly higher NO_3-$\delta^{18}O$ values compared to other sites; the average $\delta^{18}O$-NO_3 values from mainstem sites are +2.0‰ (n=26) upstream of the WWTP, -1.0‰ (n=79), +2.0 (n=26) from RM44 to Isleton, and -2.9‰ (n=70) from Rio Vista downstream. Also, there is some indication that uptake may be causing $\delta^{15}N$ and $\delta^{18}O$ values from some "RM44 to Isleton" and "Slough" samples to increase along the theoretical "uptake line" indicated by the black arrow. However, this very slight trend might also be explained by temporal and spatial variation in the original nitrate sources to different sites, later augmented by the effects of mixing with newly formed nitrate. For example, different sources of nitrate at slough versus mainstem sites is supported by the differences in the average $\delta^{18}O$ and $\delta^{15}N$ values (respectively) of samples from sites upstream of the WWTP and slough sites: +2.0‰ and +6.7‰ for upstream samples (n=26), versus -1.9‰ and +6.4‰ for slough samples (n=83).

Decreases in [NH4] downstream of SRWTP are mirrored by downstream increases in [NO3]

Fig. 26

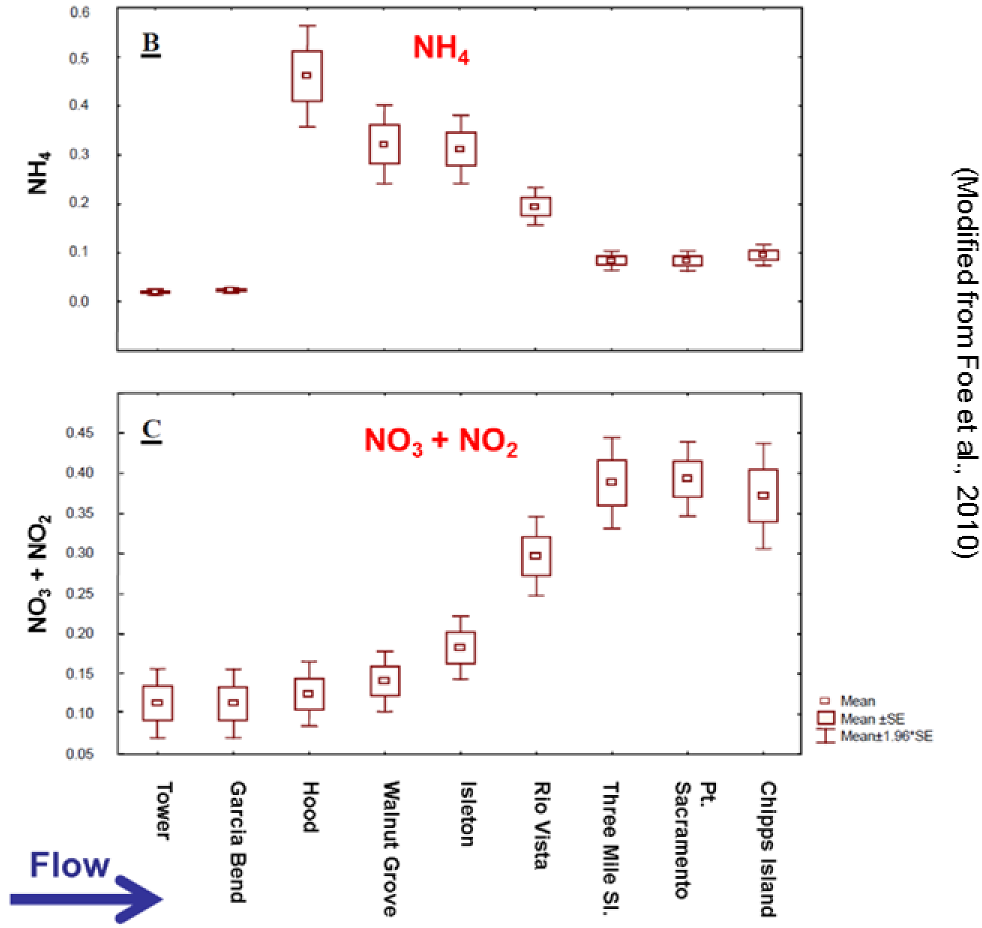

Figure 26

Comparison of the downstream average changes in NH_4 and NO_3 concentrations for all the Sacramento River and Delta samples collected as part of the Foe study in 2009-2010 (see text for details). Note that the x axis in this plot is reversed relative to the other plots in this report in that flow goes from left to right as indicated by the blue arrow, and downstream sites here are to the right. The figure is modified from Foe et al (2010).

Fig. 27

The temporal and spatial changes in the ratios of downstream NH4 loss relative to downstream NO3+NO2 gain are **NOT** mirror images.

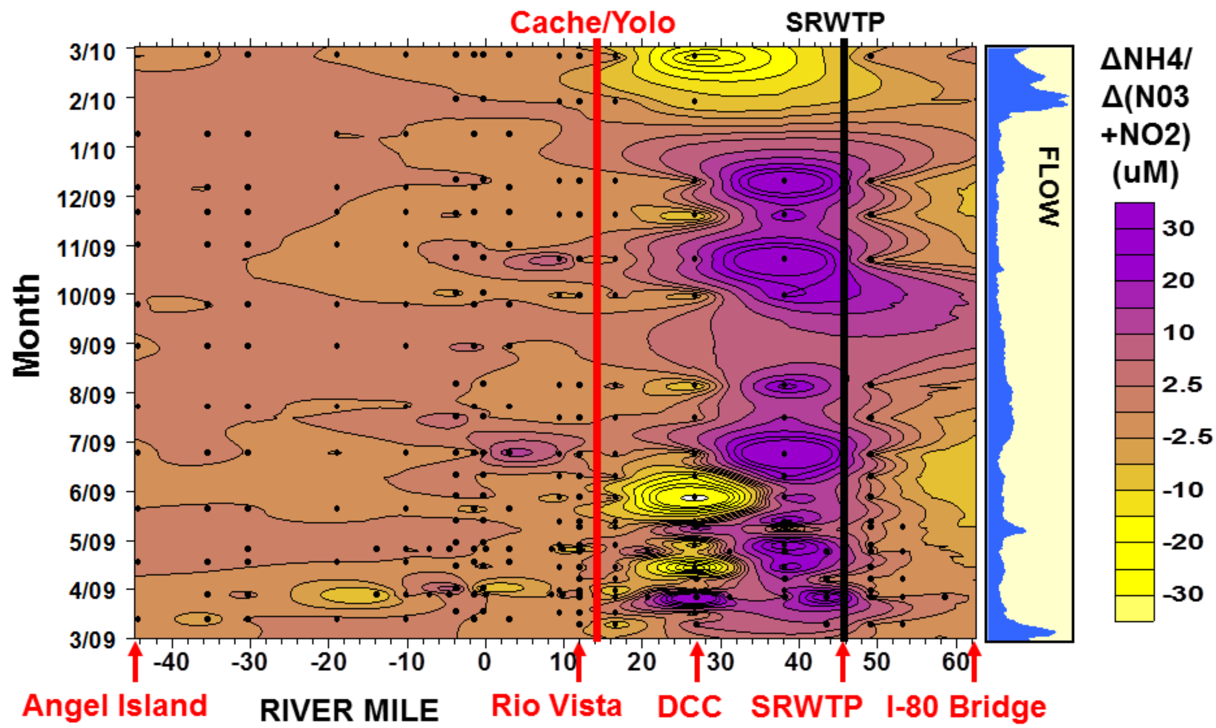

Figure 27

The downstream change (Δ) in NH_4 concentrations between adjacent mainstem Sacramento River and Delta sites, divided by the change (Δ) in NO_3+NO_2 concentrations between adjacent sites are plotted relative to river mile for all sites and dates where concentration data are available; the values are plotted at the downstream end of each reach. Note that the Δ/Δ color bar scale is not linear, with the scale expanded to better show values closer to 0. For comparison, the flow at Freeport is also shown; the black and red lines indicate the locations where SRWTP effluent and Cache/Yolo Complex water, respectively, enter the Sacramento River. The plots were made using Surfer. The largest discrepancy ratios (positive and negative), which represent a disconnect between a change in these two pools of N (NH_4 vs. NO_3+NO_2), are for adjacent sites downstream of SRWTP (RM46) and upstream of Isleton (RM17). The main conclusion is that downstream changes in NH_4 concentrations between adjacent sites are NOT mirrored by downstream changes in NO_3+NO_2 concentrations between the same adjacent sites – when the data are examined in detail.

Fig. 28

Temporal and spatial variability in the NH4 concentration.

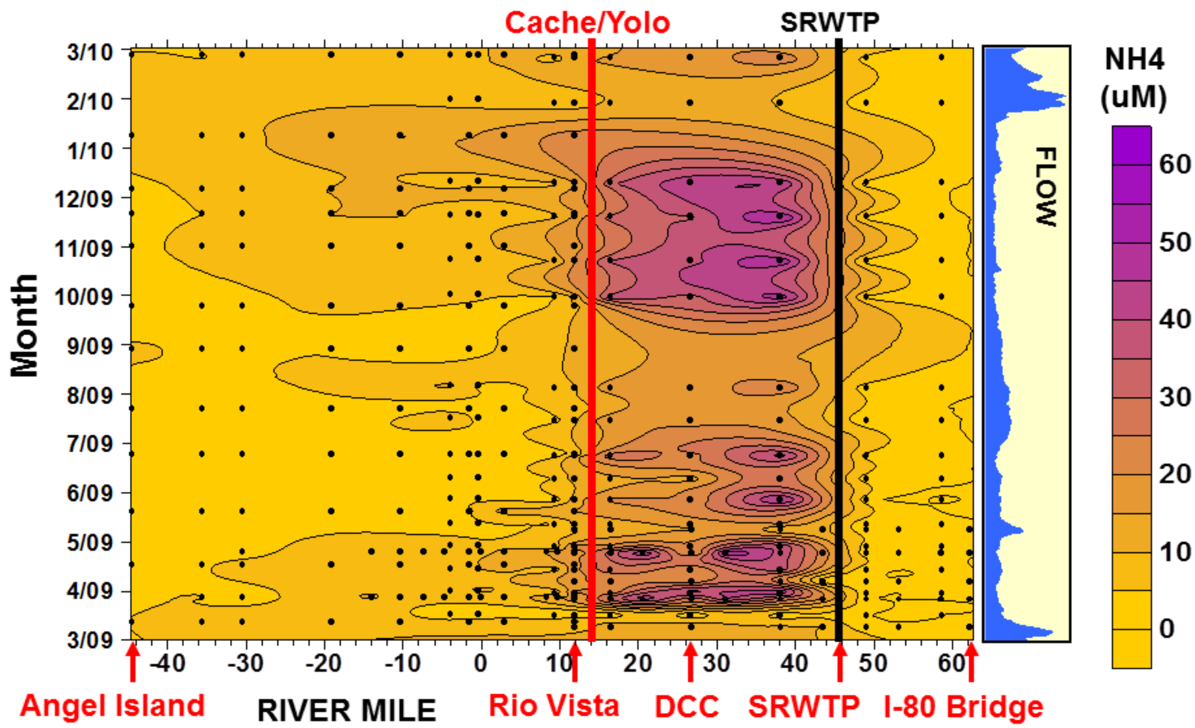

Figure 28

NH_4 concentrations are plotted relative to river mile for all sites and dates where concentration data are available. For comparison, the flow at Freeport is also shown. SRWTP effluent is discharged at about RM46 whereas the maximum NH_4 concentrations are seen at RM32 to RM38. This gradual increase in [NH_4] suggests slow downstream mixing of the effluent plume and/or degradation of effluent to form NH_4. The [NH_4] start declining rapidly downstream of RM17 (Isleton).

Fig. 29

Temporal and spatial variability in the NO3+NO2 concentration.

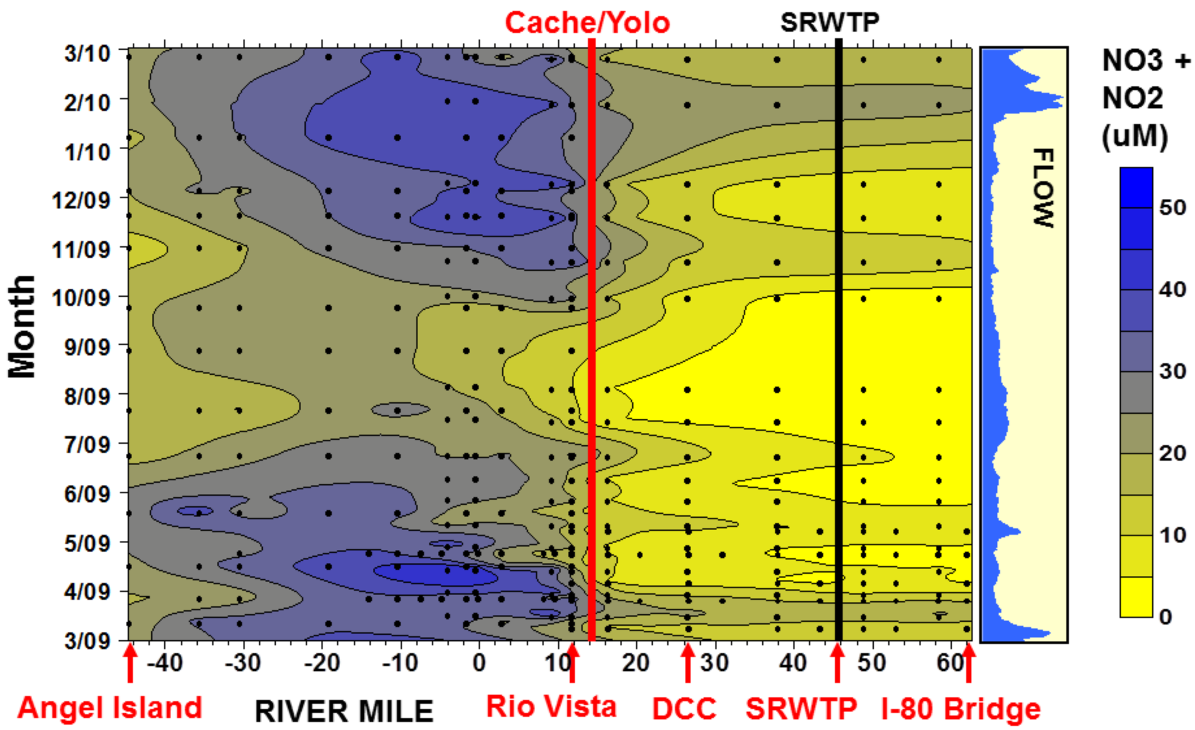

Figure 29

The sum of NO_3 and NO_2 concentrations are plotted relative to river mile for all sites and dates where concentration data are available. For comparison, the flow at Freeport is also shown. NO_3+NO_2 concentrations increase sharply downstream of Isleton (RM17) where NH_4 concentrations also begin to drop (**Figure 28**).

Fig. 30

Temporal and spatial variability in the DON concentration.

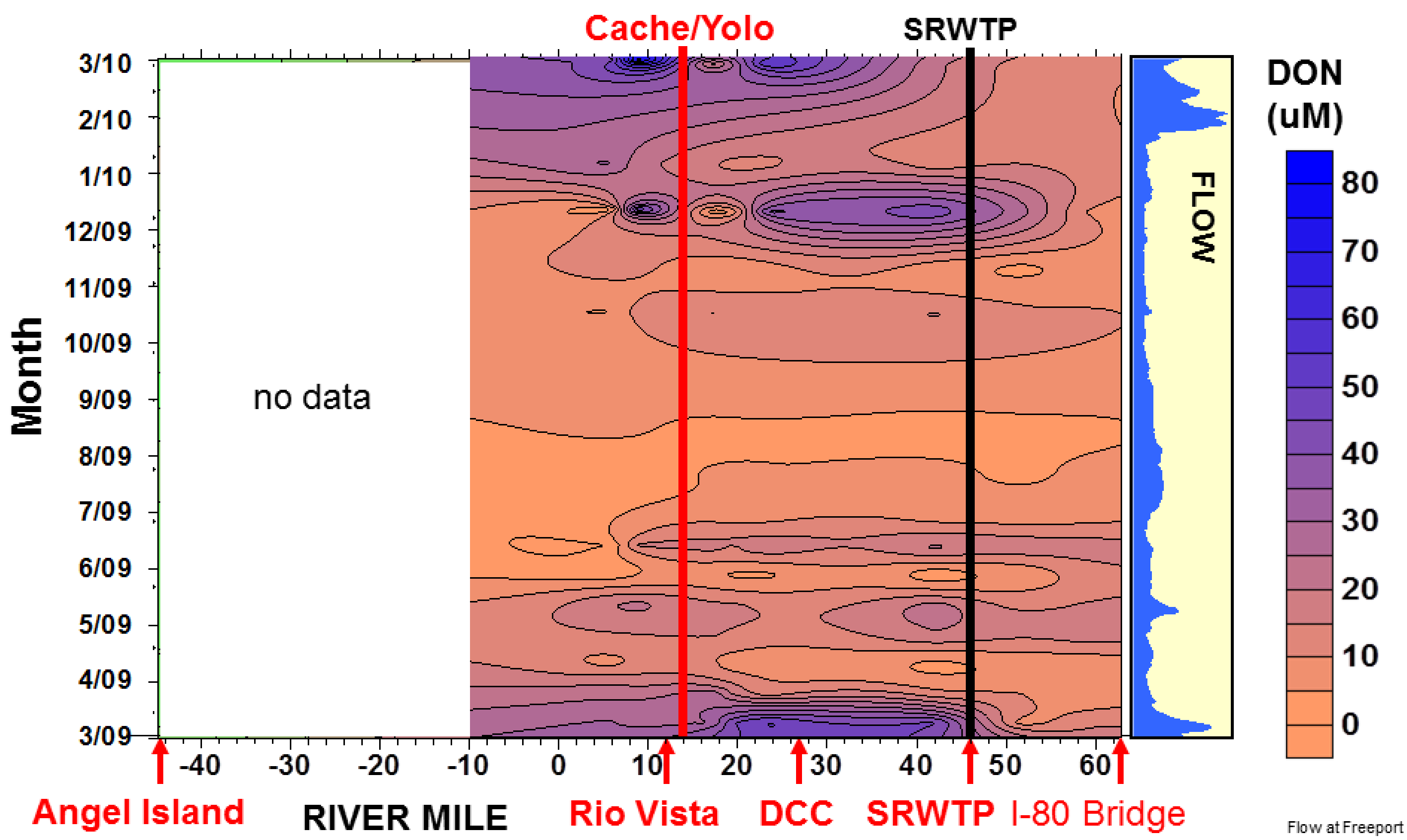

Figure 30

DON concentrations are plotted relative to river mile for all sites and dates where concentration data are available. For comparison, the flow at Freeport is also shown. DON concentrations downstream of SRWTP are high during three time periods, two associated with high flows. In general, the C:N of the DOM during the periods when [DON] is high ranges from 5-20, values that are lower than normal. The DON data are all from Foe et al (2010).

Fig. 31

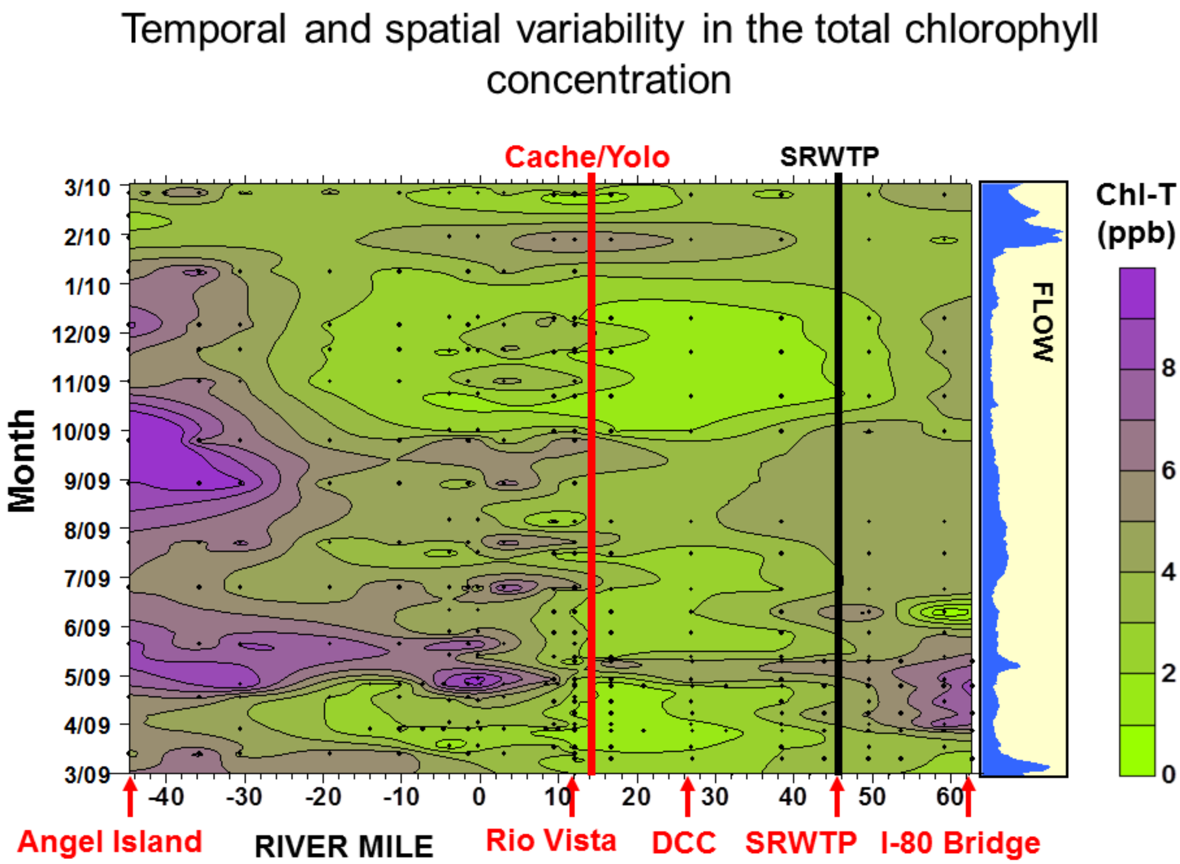

Figure 31

Total chlorophyll concentrations are plotted relative to river mile for all sites and dates where concentration data are available. For comparison, the flow at Freeport is also shown. The high concentrations observed at downstream sites in May 2009 and September 2009, and to a lesser extent in December 2009, suggest that the growth of algae at these sites and dates may be influenced by the marine-derived waters.

Fig. 32

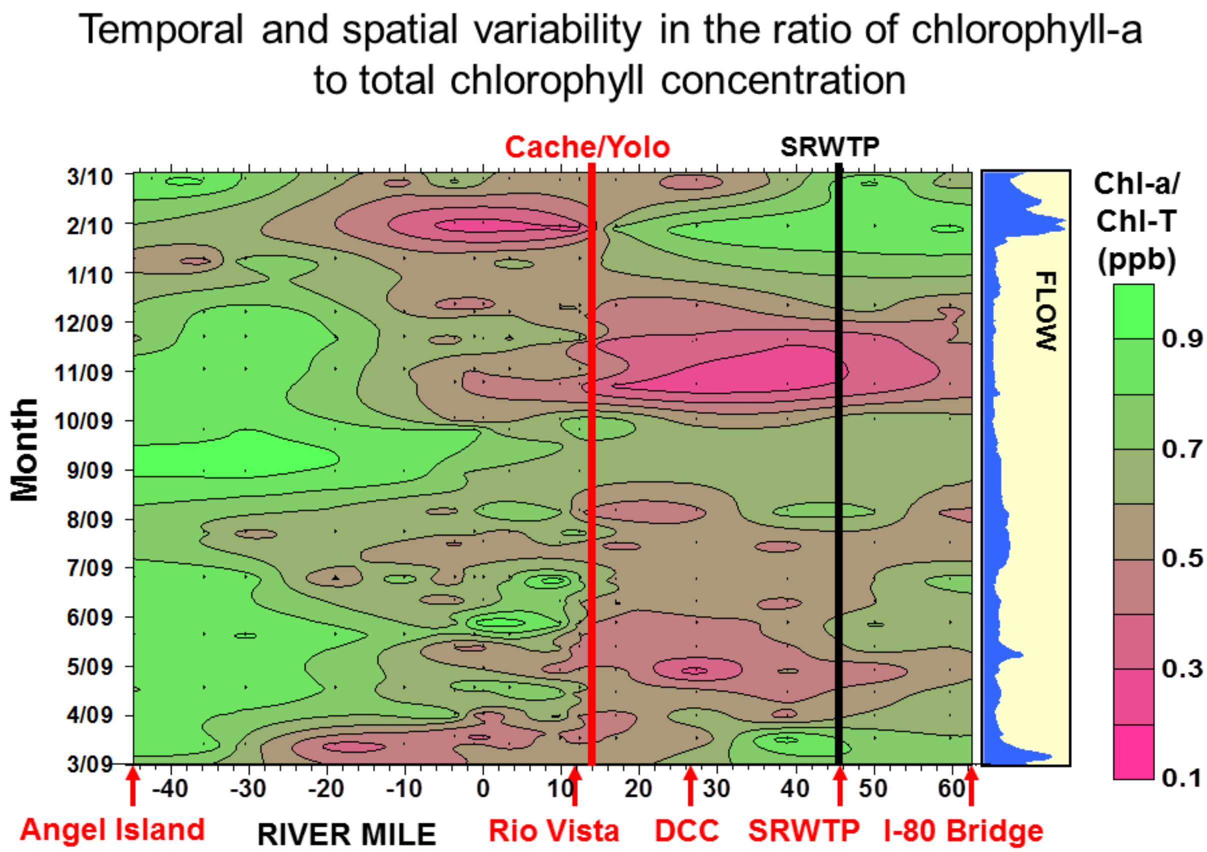

Figure 32

The ratios of chlorophyll-a to total chlorophyll concentrations (total chlorophyll = chlorophyll-a + pheophyton) are plotted relative to river mile for all sites and dates where concentration data are available. For comparison, the flow at Freeport is also shown. A higher ratio suggests a higher fraction of fresh (dominated by chlorophyll-a) algae. Note that the high ratio values observed at downstream sites in May 2009 and September 2009 correspond to the high total chlorophyll concentrations observed at these sites in Figure 31.

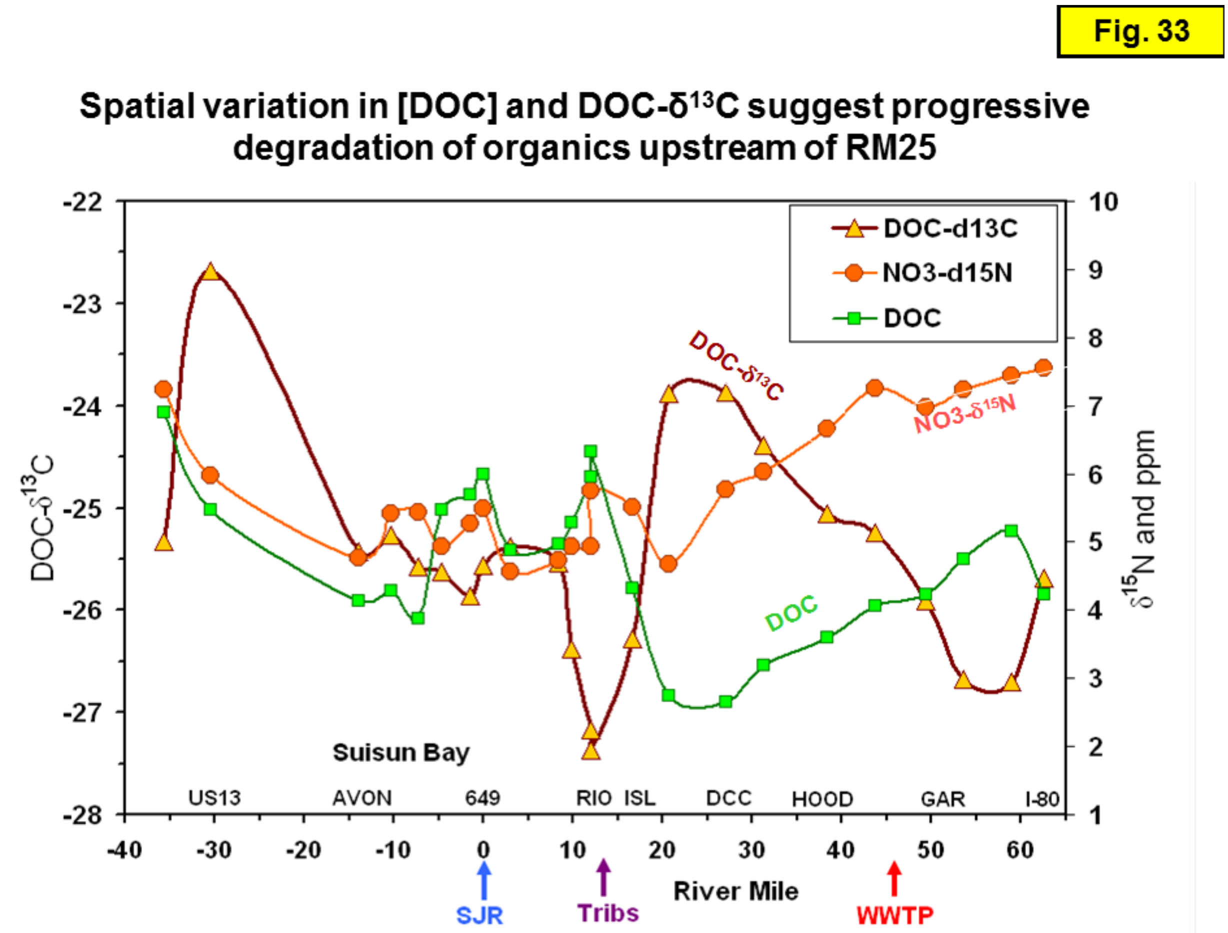

Figure 33

The general downstream decreases in [DOC] and $\delta^{15}N$-NO_3 -- and increases in DOC-$\delta^{13}C$, observed downstream to about RM20 for the March 2009 Sacramento River transect may be a consequence of bacterial uptake of DOC and NH_4 associated with nitrification that takes place downstream of the WWTP. After uptake of the more bioavailable DOC by bacteria, the residual DOC in the river is probably much less labile, with adverse consequences for bacteria-based food webs downstream of RM25. The inversion points for DOC concentration and DOC-$\delta^{13}C$, and "dip" in $\delta^{15}N$-NO_3, occur at about the location (~RM20) where the tide reversed during sampling (see Figure 11 and discussion in the report). The abrupt changes at Rio Vista probably also reflect the effect of another tidal reversal during sampling (see Figure 11), perhaps resulting in poorly mixed influxes of water with a different composition from the Cache/Yolo Complex sloughs.

Fig. 34

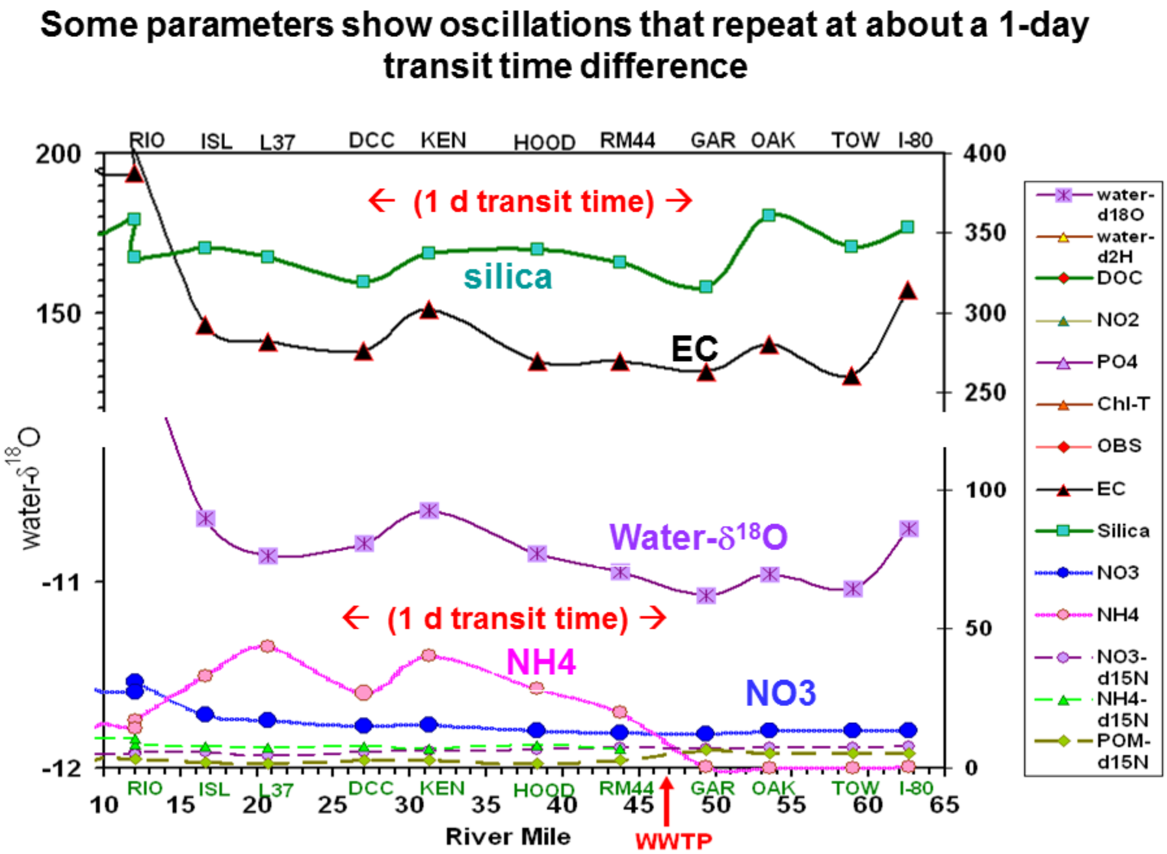

Figure 34

Conservative tracers of water sources like EC (electrical conductivity), δ18O-water, and silica for March 2009 samples show similar downstream oscillations in composition, suggesting temporal differences in the effluent loads (i.e., variable dilution with upstream water). With the exception of the dip in [NH4] at DCC (RM27), which is about 1-day transit time from SRWTP, the other non-conservative parameters do not appear to show significant oscillations. Hence, a likely explanation for the frequently observed dip in [NH4] at the DCC site is that it is a sampling artifact, caused by sampling a parcel of water at DCC with a relatively low % effluent. On most transects, sampling starts near the SRWTP at close to high tide when the effluent is most diluted, and since under many flow conditions water at the DCC site has traveled ~1day since passing the SRWTP, the water at this site represents the dilute "high tide" parcel from the previous day. The [NO3] downstream of SRWTP is minimally affected by changes in % effluent because the load of NO3 from SRWTP is normally much smaller than the load from upstream of SRWTP. Also, nitrification, the main process affecting [NO3] in the Sacramento River is not limited by substrate (NH4) concentration.

Fig. 35

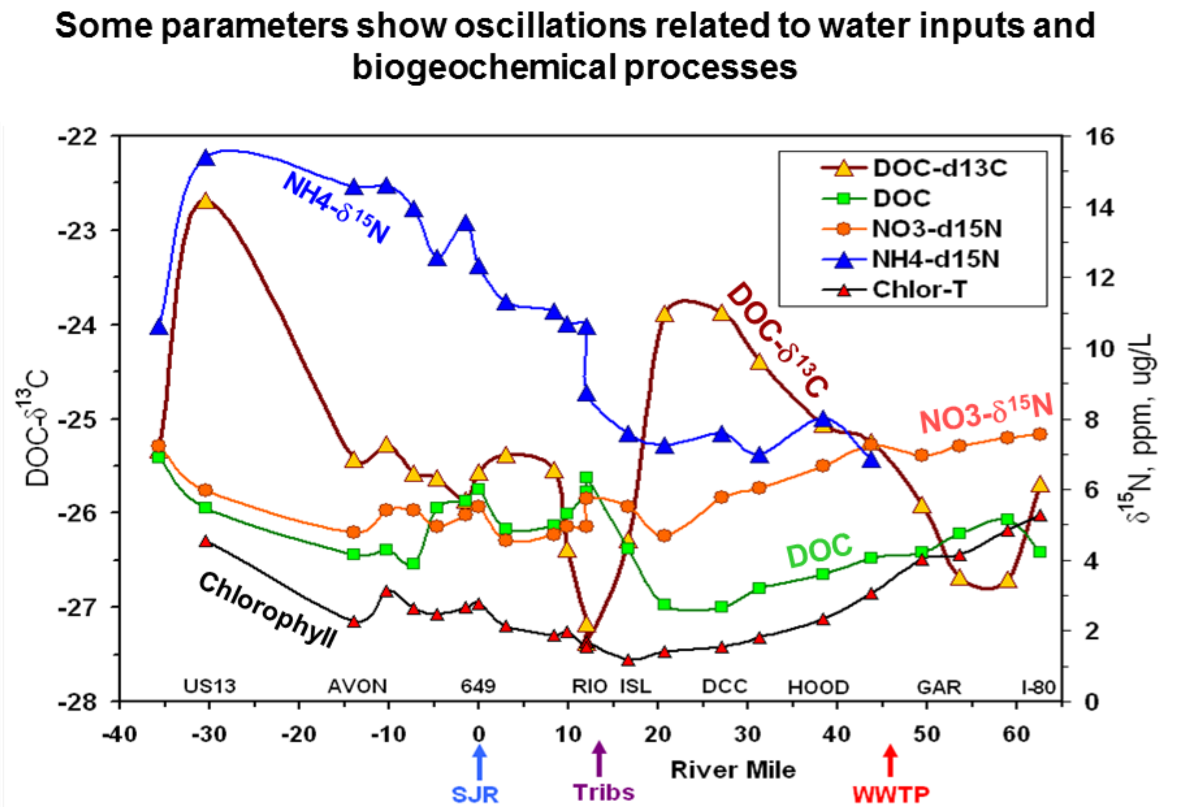

Figure 35

Many parameters measured for March 2009 samples do NOT oscillate in composition -- but instead show gradational downstream changes in composition indicative of processes (such as nitrification) relatively unaffected by changes in effluent loads, except for locations that receive significant amounts of new water and constituents from the Cache/Yolo Complex tributaries like RM12 (Rio Vista). The downstream inverse trends in [DOC] and DOC-δ^{13}C suggest degradation of organic matter.

Fig. 36

Typical compositional values of major organic matter sources

Organic matter source	$\delta^{13}C$ (‰)	$\delta^{15}N$ (‰)	$\delta^{34}S$ (‰)	C:N (at.)
Heterotrophic bacteria	Similar to substrate	-15 to +20	-15 to +20	4 to 8
Algae		-15 to +20	-10 to +33	
Periphyton	-35 to -18 (-47 to -8)			5 to 12
Phytoplankton	-32 to -23 (-42 to -19)			5 to 8
Macrophytes*	-27 to -20	-15 to +20	-10 to +33	10 to >50
Soil organic matter		+2 to +5	0 to +5 (-30 to +35)	8 to >25
C3	-27 (-32 to -22)			
C4	-13 (-16 to -9)			
Terrestrial plants		+3 to 7 (-10 to +10)	0 to +5 (-10 to +20)	15 to >50
C3	-27 (-32 to -22)			
C4	-13 (-16 to -9)			

* excluding bryophytes

(from Finlay and Kendall, 2007)

Figure 36

The typical values and ranges in the $\delta^{13}C$, $\delta^{15}N$, and $\delta^{34}S$ of the major organic matter sources to aquatic ecosystems are shown without parentheses; the ranges of observed values are in parentheses. The data are from Table 10.2 in Finlay and Kendall (2007).

Fig. 37

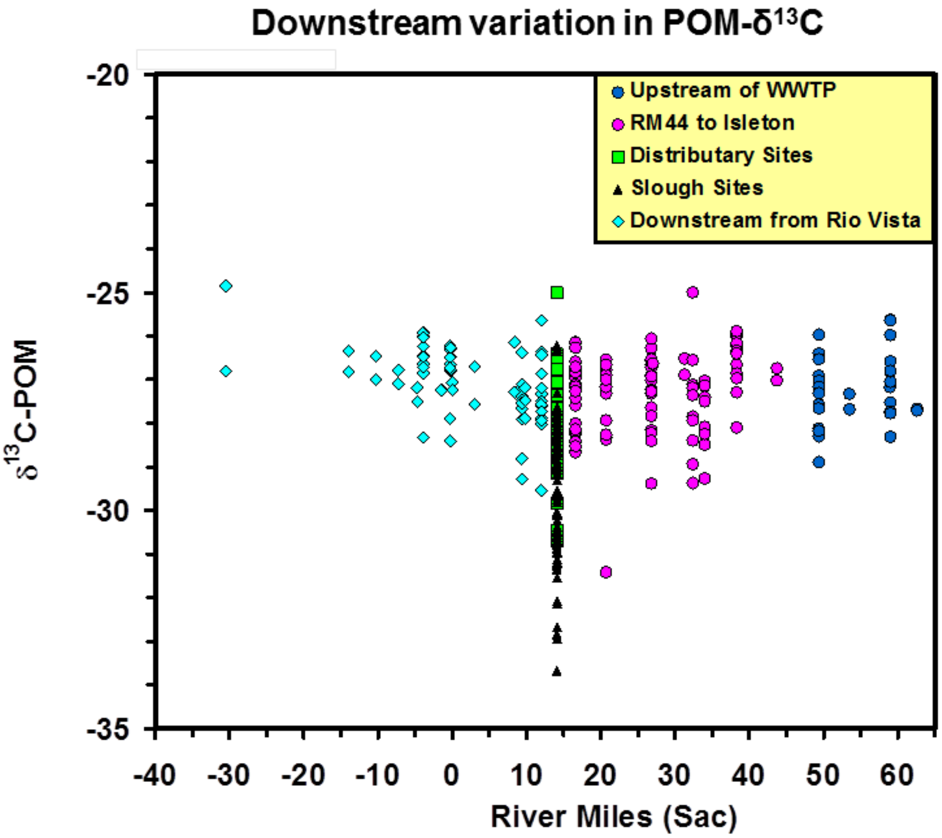

Figure 37
POM-$\delta^{13}C$ for samples from different sections of the transects and site types are plotted relative to RM. The data for the Cache/Yolo Complex tributaries (sloughs) and the Miner and Steamboat Slough distributaries are plotted at RM14 because that is where the Cache Slough converges with the Sacramento River. Many of the slough samples have much lower $\delta^{13}C$ values than samples from upstream or downstream of where the Cache/Yolo Slough converges with the Sacramento River, probably indicating more drawdown of the DIC pool in the semi-restricted Cache/Yolo Complex tributaries due to more intense photosynthesis and algal growth in this section of the Delta than in other sections.

Fig. 38

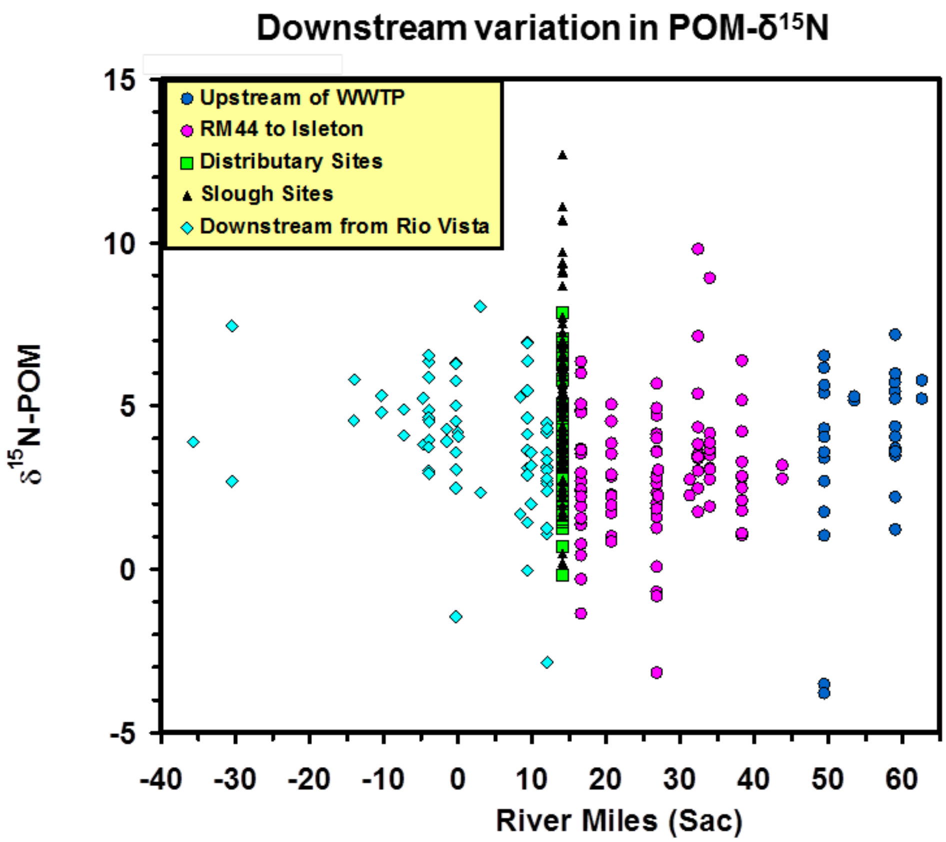

Figure 38
POM-$\delta^{15}N$ for samples from different sections of the transects and site types are plotted relative to RM. The data for the Cache/Yolo Complex tributaries (sloughs) and the Miner and Steamboat Slough distributaries are plotted at RM14 because that is where the Cache Slough converges with the Sacramento River. Many of the Slough samples have much higher $\delta^{15}N$ values than samples from upstream or downstream of where the Cache/Yolo Slough converges with the Sacramento River, probably indicating more uptake of NH_4 (and more drawdown of the NH_4 pool) and hence more fractionation of the resulting NH_4 in the semi-restricted Cache/Yolo Complex sloughs due to more intense photosynthesis and algal growth in this section of the Delta than in other sections.

Fig. 39

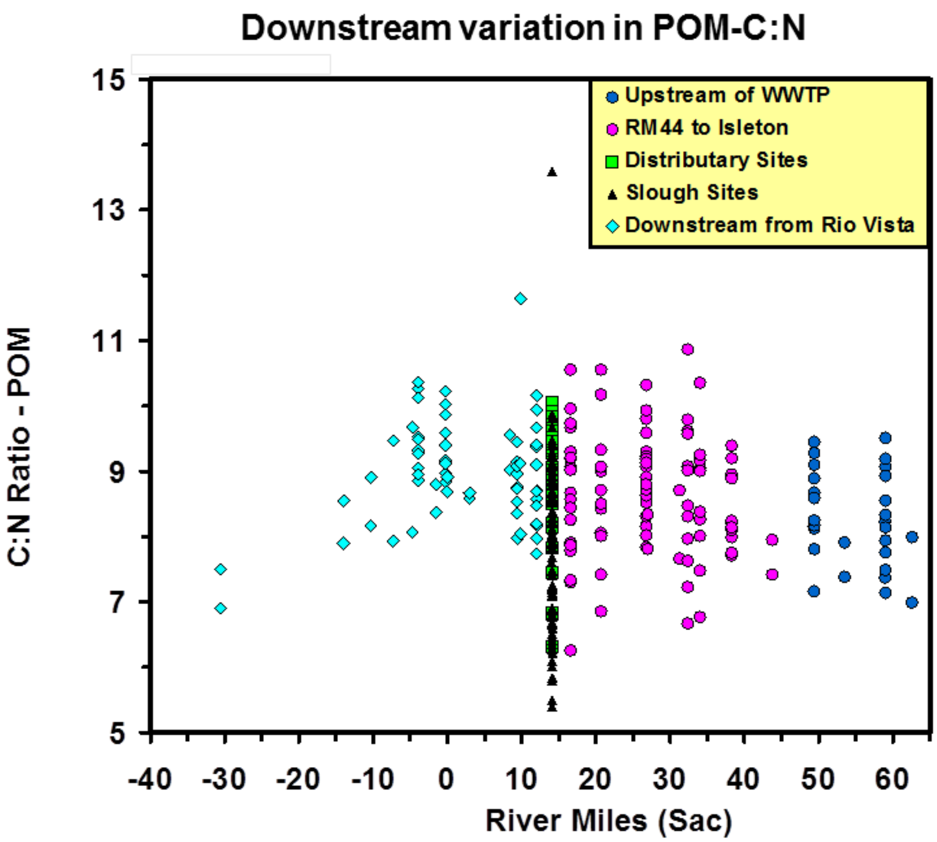

Figure 39
POM-C:N for samples from different sections of the transects and site types are plotted relative to RM. The data for the Cache/Yolo Complex tributaries (sloughs) and the Miner and Steamboat Slough distributaries are plotted at RM14 because that is where the Cache/Yolo Slough converges with the Sacramento River. Many of the Slough samples have much lower C:N than samples from upstream or downstream of where the Cache/Yolo Slough converges with the Sacramento River, indicating that the POM contains a higher proportion of algae and bacteria than the other samples.

Fig. 40

C:N and δ13C values of POM show that POM in the sloughs are more algal-dominated than at mainstem sites

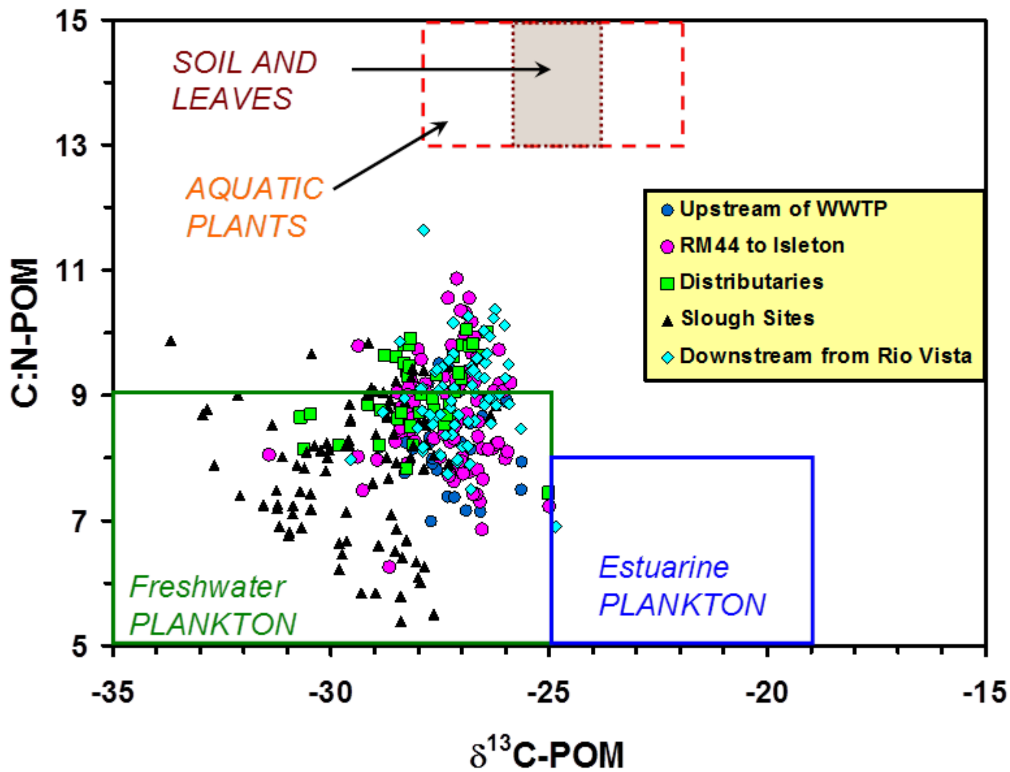

Figure 40

POM-δ^{13}C for samples collected from different sections of the transects and site types are plotted relative to POM-C:N. Box boundaries for different POM sources (plankton, aquatic plants, soil and leaves) are based on data from Cloern et al. 2002), Finlay and Kendall (2007), and unpublished USGS data from the San Francisco Estuary (SFE). Despite appearances, the average C:N of slough POM samples is 7.9 ± 1.2, only slightly lower than the average C:N of POM from RM44 to Isleton, which is 8.6 ± 0.9. The Lindsey and Toe Drain slough sites have only slightly lower C:N values than the other sloughs (7.6 vs. 8.3), so site location does not explain the group of slough sites with C:N values of 5-7 on the plot. But examination of the data in the downloadable Excel file shows that most of the low C:N values are for samples collected May through September during the dry season when there are few storms events which carry terrestrial runoff into the river.

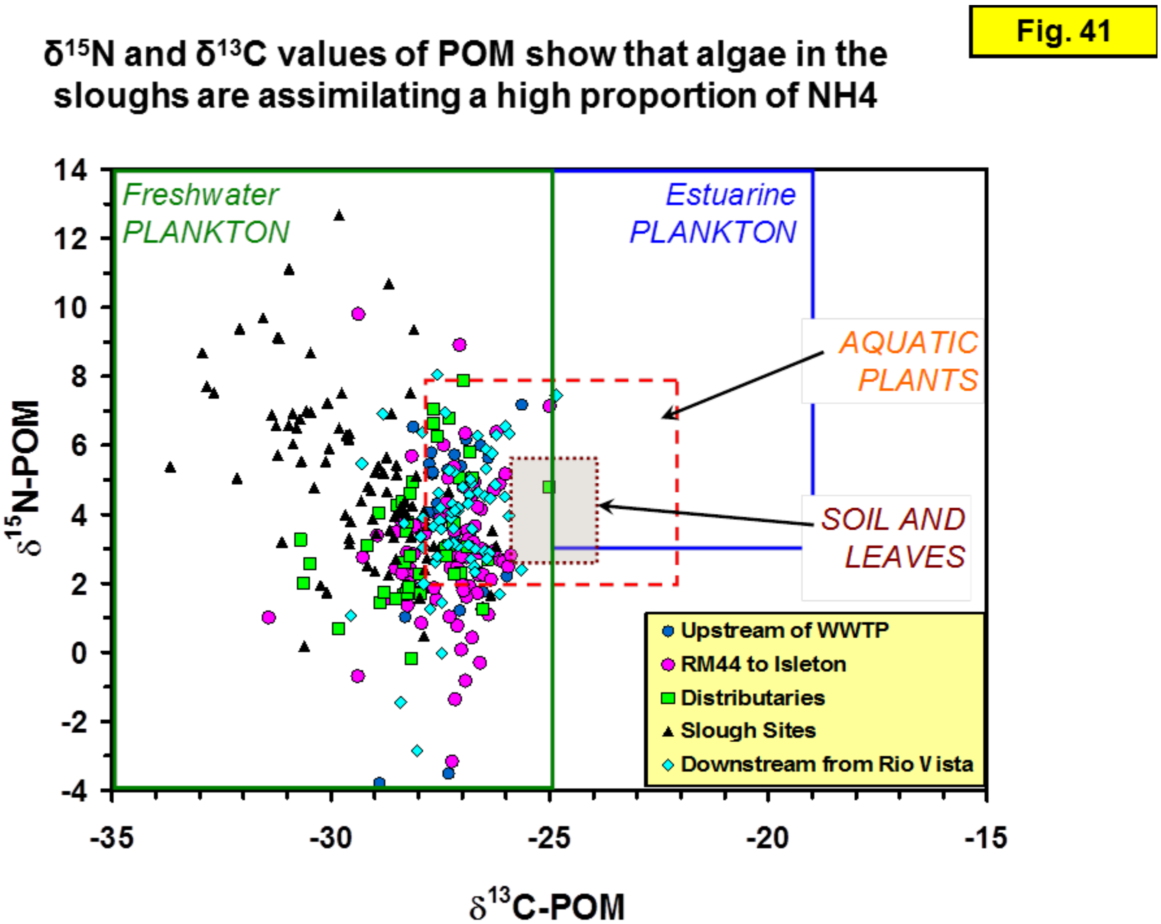

Figure 41

POM-δ^{15}N for samples collected from different sections of the transects and site types are plotted relative to POM-δ^{13}C. Box boundaries for different POM sources (plankton, aquatic plants, soil and leaves) are based on data from Cloern et al. (2002), Finlay and Kendall (2007), and unpublished USGS data from the SFE. The average POM-δ^{15}N for slough samples is +5.2 ± 2.4‰, which is considerably higher than the average POM-δ^{15}N from RM44 to Isleton, which is +2.9 ±2.2‰. The average POM-δ^{13}C for slough samples is -29.5 ±1.7‰, which is considerably lower than the average POM-δ^{13}C from RM44 to Isleton, which is -27.3 ±1.0‰.

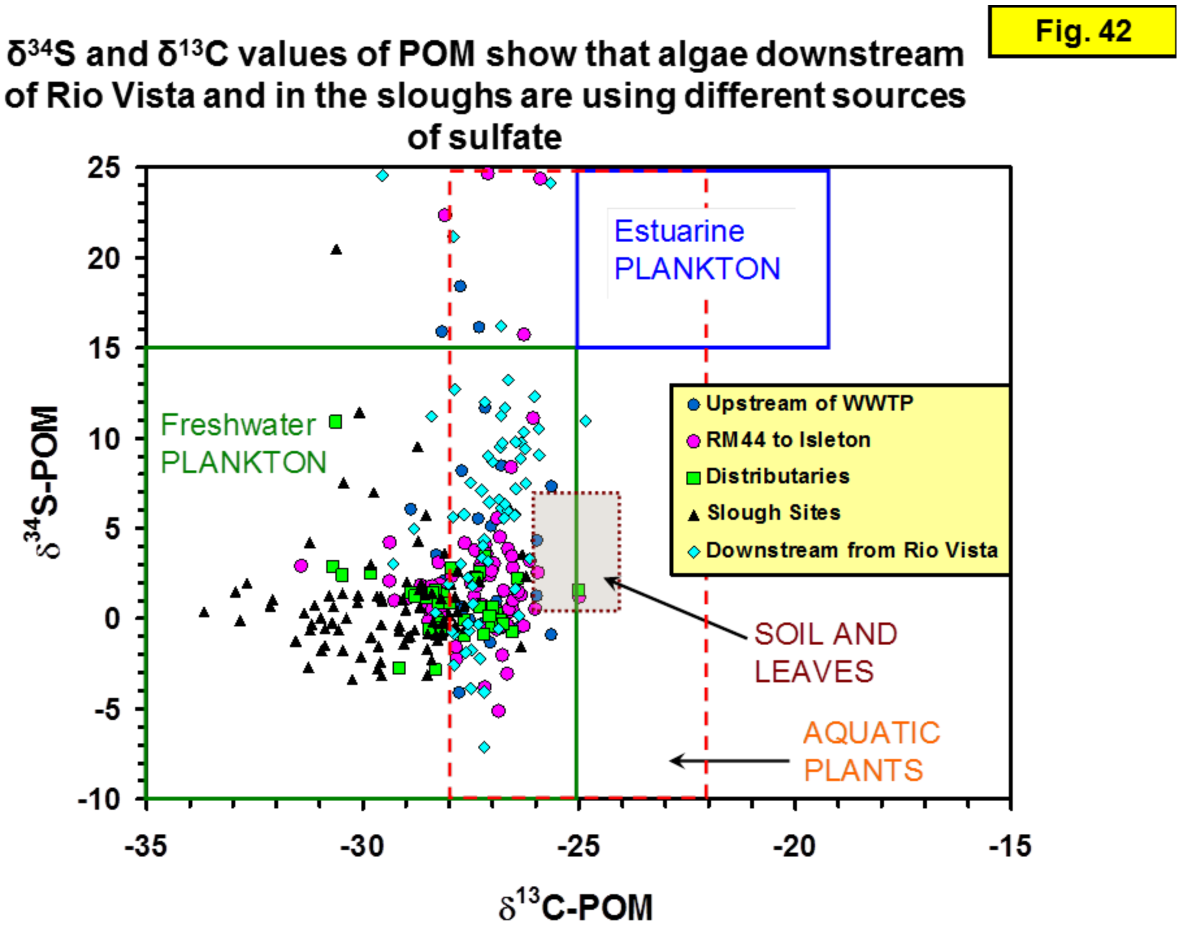

igure 42
POM-δ^{13}C for samples collected from different sections of the transects and site types are plotted relative to POM-δ^{34}S. Box boundaries for different POM sources (plankton, aquatic plants, soil and leaves) are based on data from Cloern et al. (2002), Finlay and Kendall (2007), and unpublished USGS data from the SFE. Samples from the Cache/Yolo Complex tributaries and sloughs are grouped under "Slough sites" on this plot. The average POM-δ^{34}S of slough samples is +1.3 ±7.1‰, which is not significantly different from the average POM-δ^{34}S from RM44 to Isleton, which is +2.4 ±4.9‰. The high POM-δ^{34}S for sites upstream of Rio Vista are suspicious and merit investigation.

Fig. 43

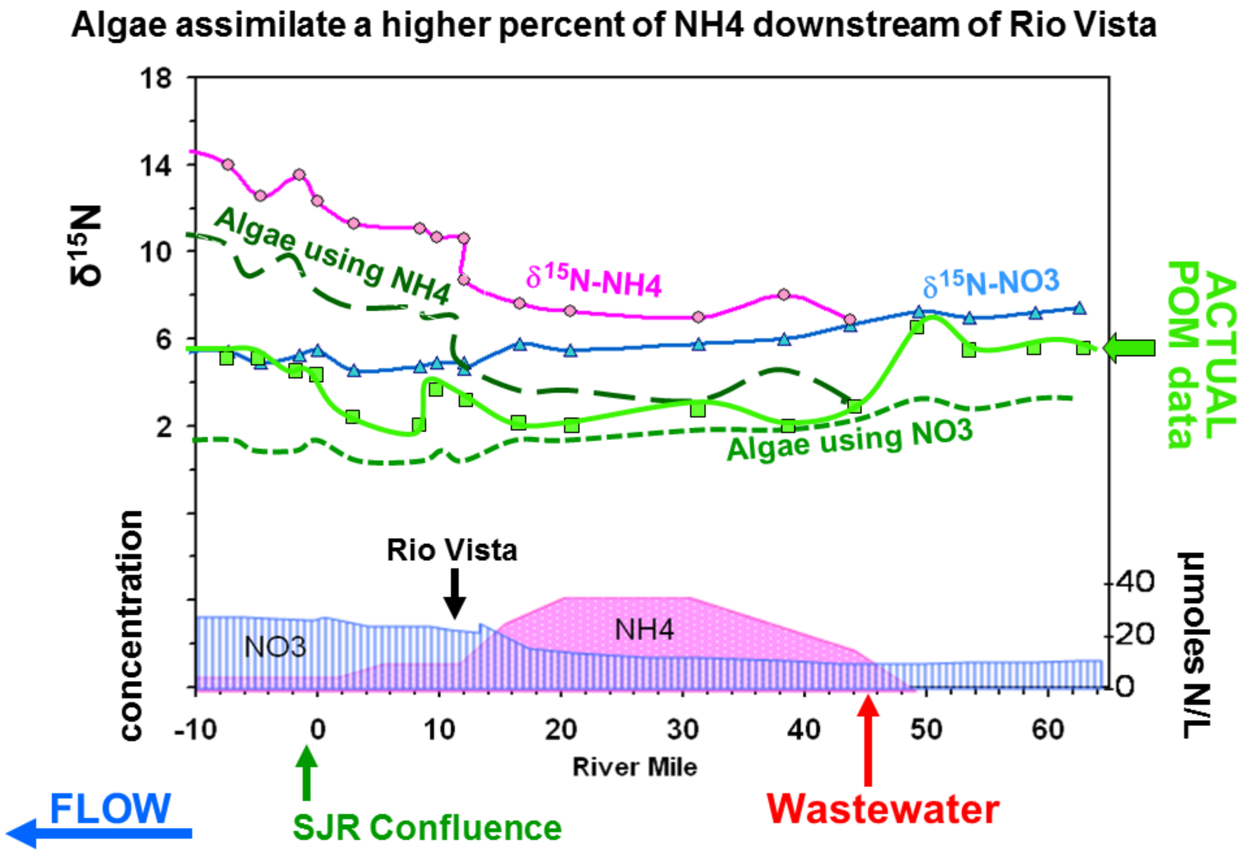

Figure 43

The March 2009 $\delta^{15}N$ values for NH_4, NO_3, and POM (solid lines) are compared with calculated $\delta^{15}N$ values for algae assuming a 4‰ fractionation (dashed lines) for both NH_4 uptake (denoted "algae using NH4") and NO_3 uptake (denoted "algae using NO3"). Data for the DCC site (RM27) are omitted due to anomalously low NH_4 concentrations. The actual POM data plot between calculated values for algae data for NO_3 and NH_4 assimilation. In general, between the SRWTP and RM15, the actual POM data are a better match to the calculated algae data for NO_3 assimilation downstream, and the calculated algae data for NH_4 assimilation are generally a better fit downstream of RM15.

Fig. 44

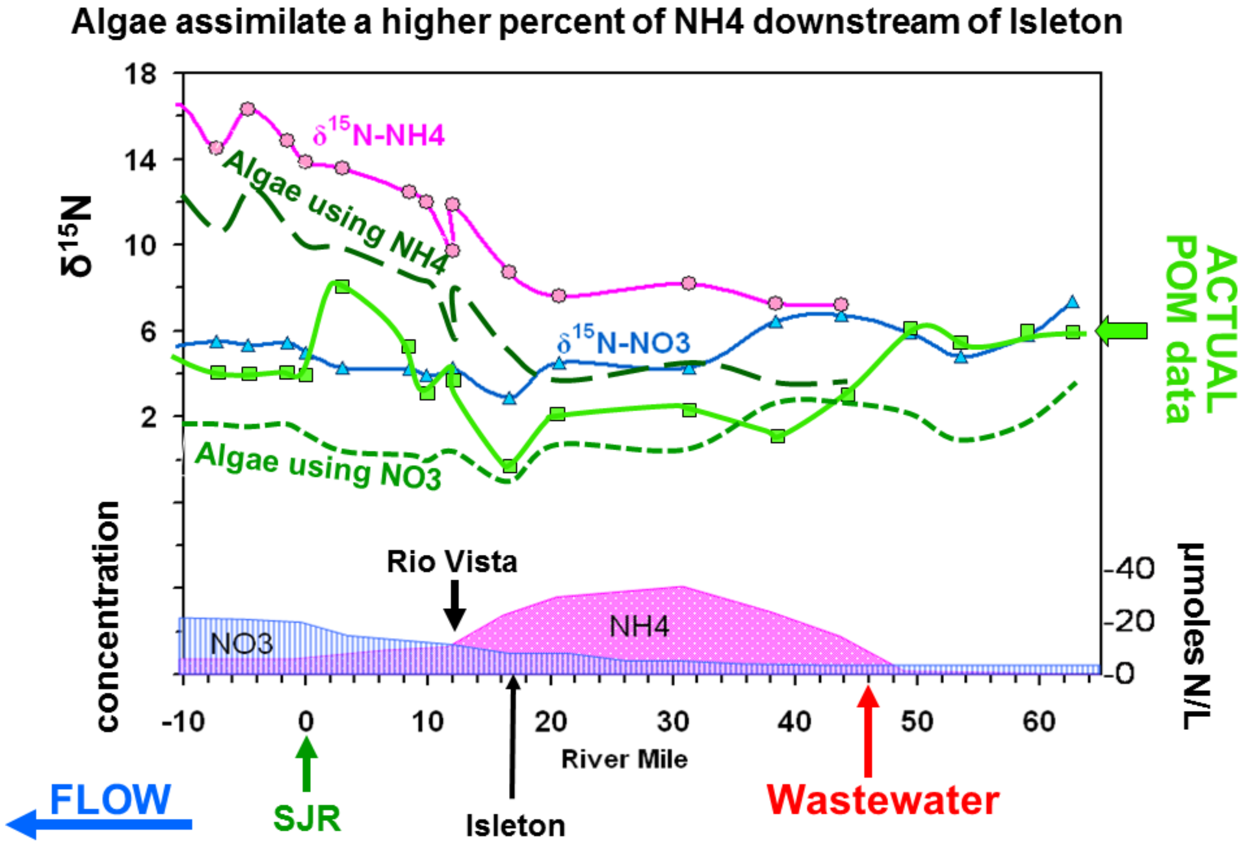

Figure 44

The April 2009 δ^{15}N values for NH_4, NO_3, and POM (solid lines) are compared with calculated δ^{15}N values for algae assuming a 4‰ fractionation (dashed lines) for both NH_4 uptake (denoted "algae using NH4") and NO_3 uptake (denoted "algae using NO3"). Data for the DCC site (RM27) are omitted due to anomalously low NH_4 concentrations. Data from April 2009 are more complex than for March 2009. The abrupt trend upward in δ^{15}N-POM at the same location (RM17) as the upward trend in δ^{15}N-NH_4 is evidence of increasing proportion of NH_4 assimilation downstream of this location, and the sharp drop to lower values (RM0) is probably reflecting a switch back to dominant NO_3 use downstream of this location.

Fig. 45

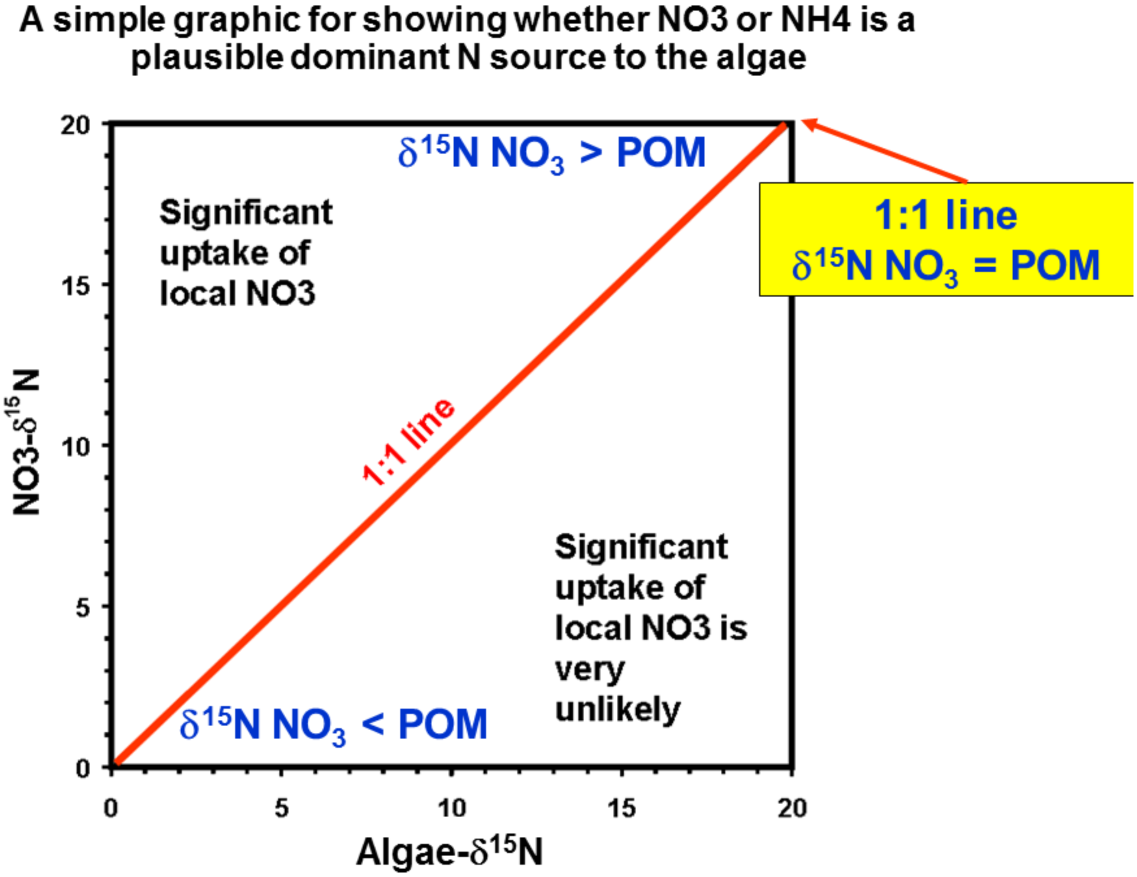

Figure 45

This plot provides a useful graphical means for showing whether the $\delta^{15}N$ data for algae (i.e., only data for POM samples with C:N ≤ 9.0) are consistent or not consistent with NO_3 as dominant N source. The red 1:1 line denotes when the $\delta^{15}N$ values of algae and NO_3 are the same. Because of isotope fractionation, algae assimilating NO_3 should plot above line for samples, and algae that were not assimilating NO_3 (and thus were presumably assimilating NH_4) would plot below the line. If the algae consumed all the NO_3, there would be no isotope fractionation and the algae would plot on the line.

Fig. 46

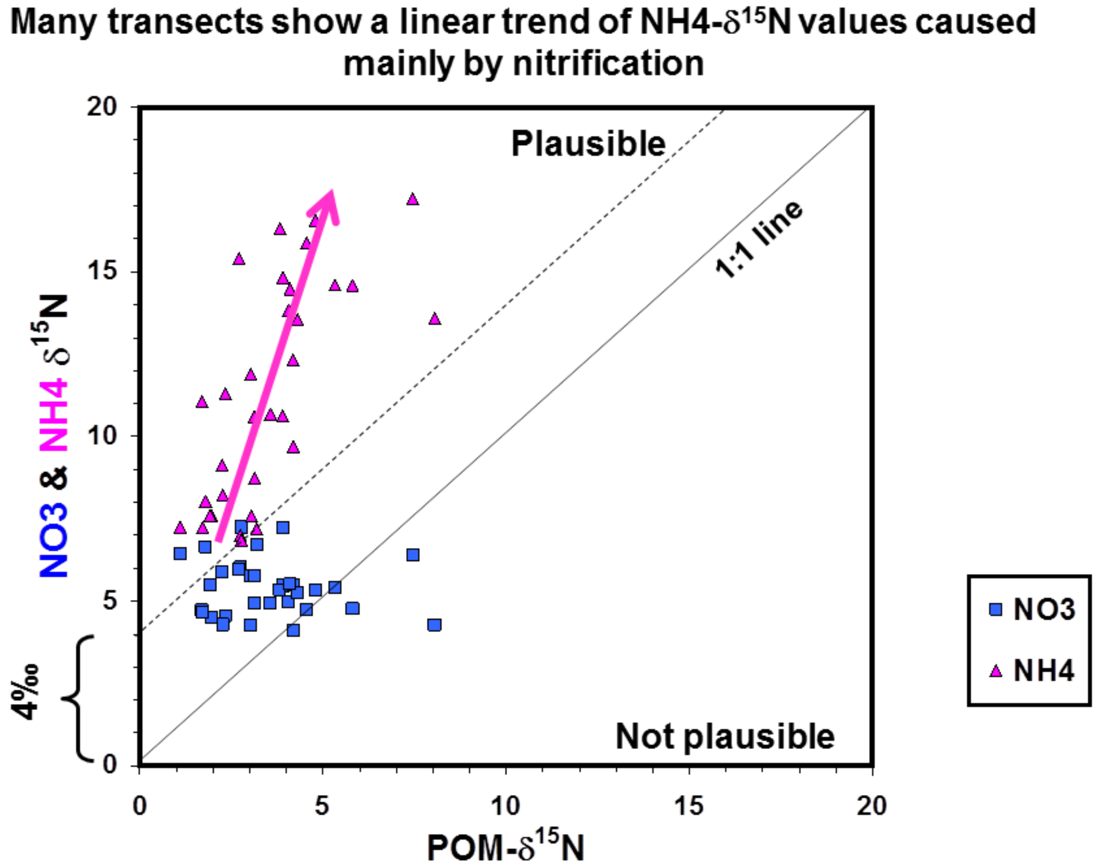

Figure 46
The δ^{15}N values of NO_3 and NH_4 for March and April 2009 of algae-dominated POM samples (C:N $\leq$ 9) collected along the Sacramento River transects are plotted relative to δ^{15}N-POM (see **Figure 45** for plot explanation). Note that the axis labels and symbols are color coded (NH_4: pink; NO_3: blue). The dashed line above the 1:1 line represents the theoretical position of data if all the N in algae was derived entirely from ambient NO_3, with a typical 4‰ isotope fractionation. Since all the δ^{15}N-NH_4 values (pink) plot well above the 1:1 line, NH_4 is a plausible dominant source of N to algae. Since almost all of the NO_3-δ^{15}N values (blue) plot either below the 1:1 line or < 4‰ above the line, NO_3 is **not** a plausible dominant source of N to algae. The pink arrow shows the linear trend of increasing δ^{15}N-POM and values with decreasing NH_4 concentration (see **Figure 17** and **Figure 18**).

Fig. 47

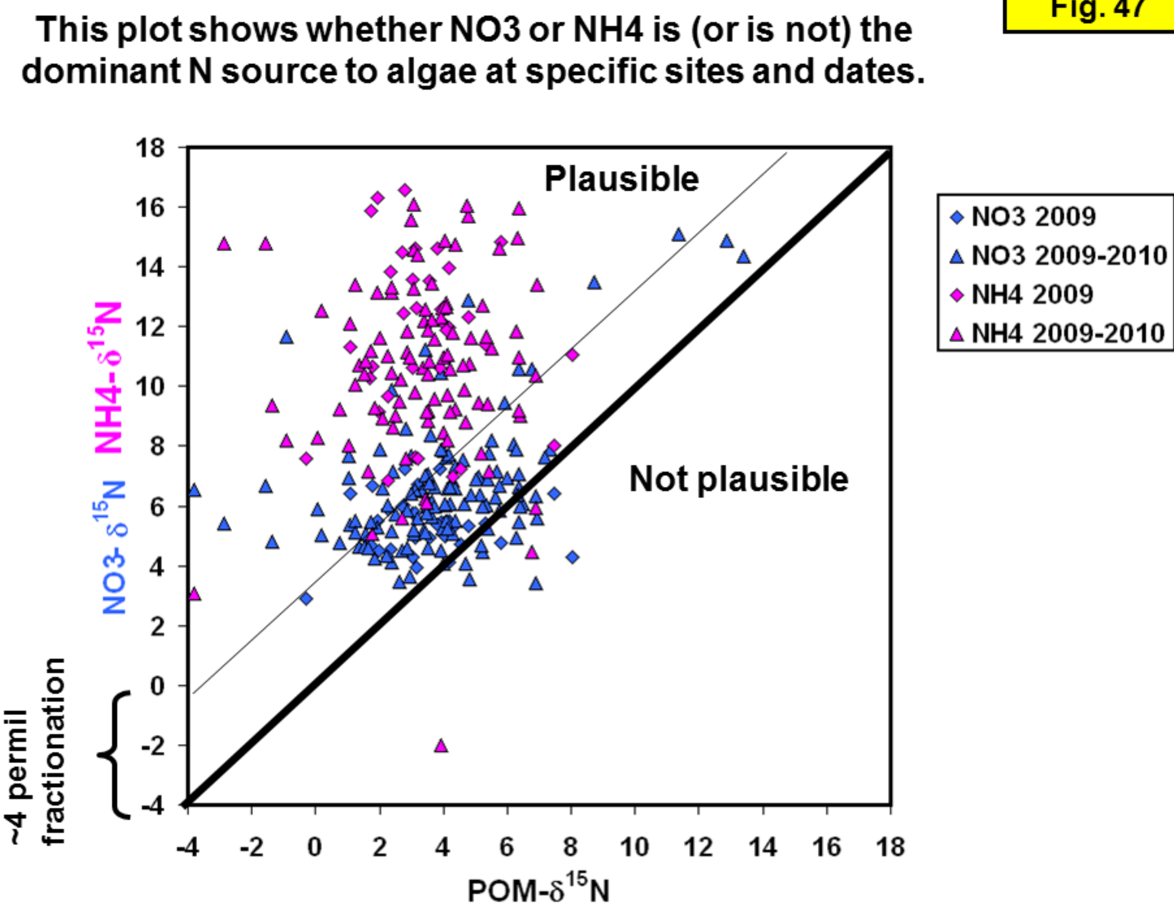

Figure 47

This plot shows all the $\delta^{15}N$ data for samples collected during the 2009-2010 transects that have algae-dominated POM with C:N ≤ 9. Note that the axis labels and symbols are color coded (NH_4: pink; NO_3: blue). Sample shape denotes samples from just the two "Dugdale transects" (denoted "2009"), and ones from the "Foe transects" (denoted "2009-2010"). Like the previous plot, for most samples, NH_4 is the most plausible dominant source of N to algae. However, for samples where both the NH_4-$\delta^{15}N$ and the NO_3-$\delta^{15}N$ values plot above the 4‰ fractionation line (thin black line), contributions of NH_4 and NO_3 to algal uptake may be sub-equal (assuming that a 4‰ fractionation is a reasonable assumption for both NH_4 and NO_3, which is still unresolved).

Fig. 48

Downstream changes in the %NH4 assimilated by algae in August 2009

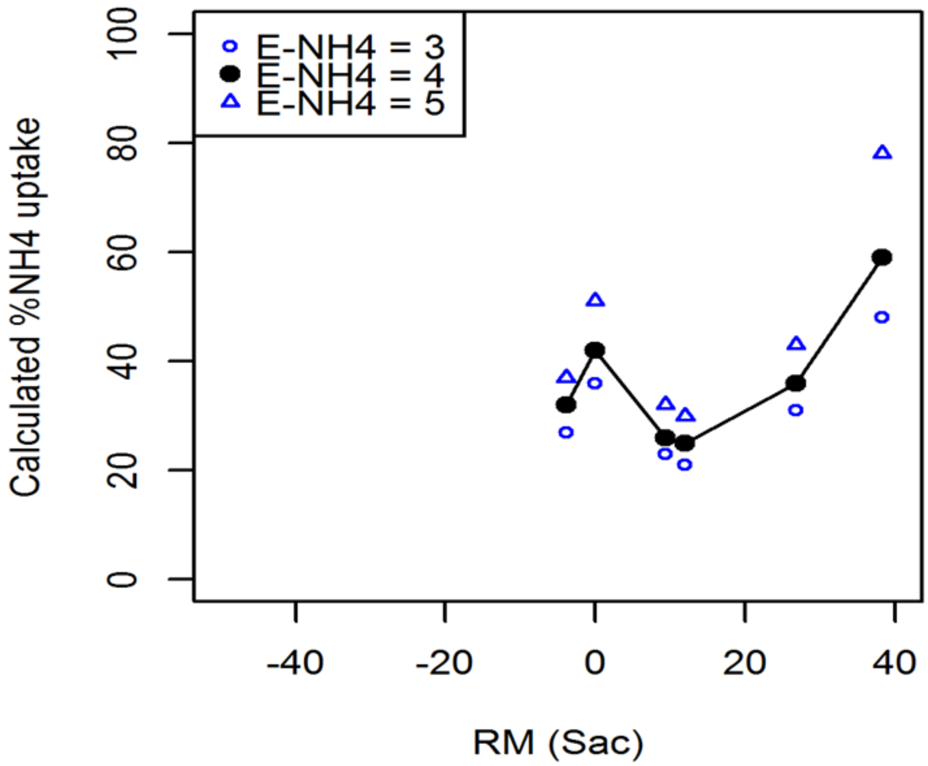

Figure 48

This plot shows an example of preliminary calculations of the %NH_4 uptake by algae along the Sacramento River between RM38 (Hood) and RM-5 (US 649), for data from the August 2009 Foe transect. The calculations assumed a NO_3 fractionation factor of 4, and three different NH_4 fractionation factors (**ε** = 3, 4, 5). Calculations for sites downstream of RM-3 did not give good model fits, for reasons still being investigated. This plot shows that the % of NH_4 (as opposed to NO_3) assimilated decreases from ~60% at RM38 to ~30% at RM12 (Rio Vista), and then slightly increases where the San Joaquin River converges with the Sacramento River (RM0).

Fig. 49

Locations of sampling sites near the confluence area where waters from the Cache/Yolo Complex tributaries converge with the Sacramento River and its distributaries

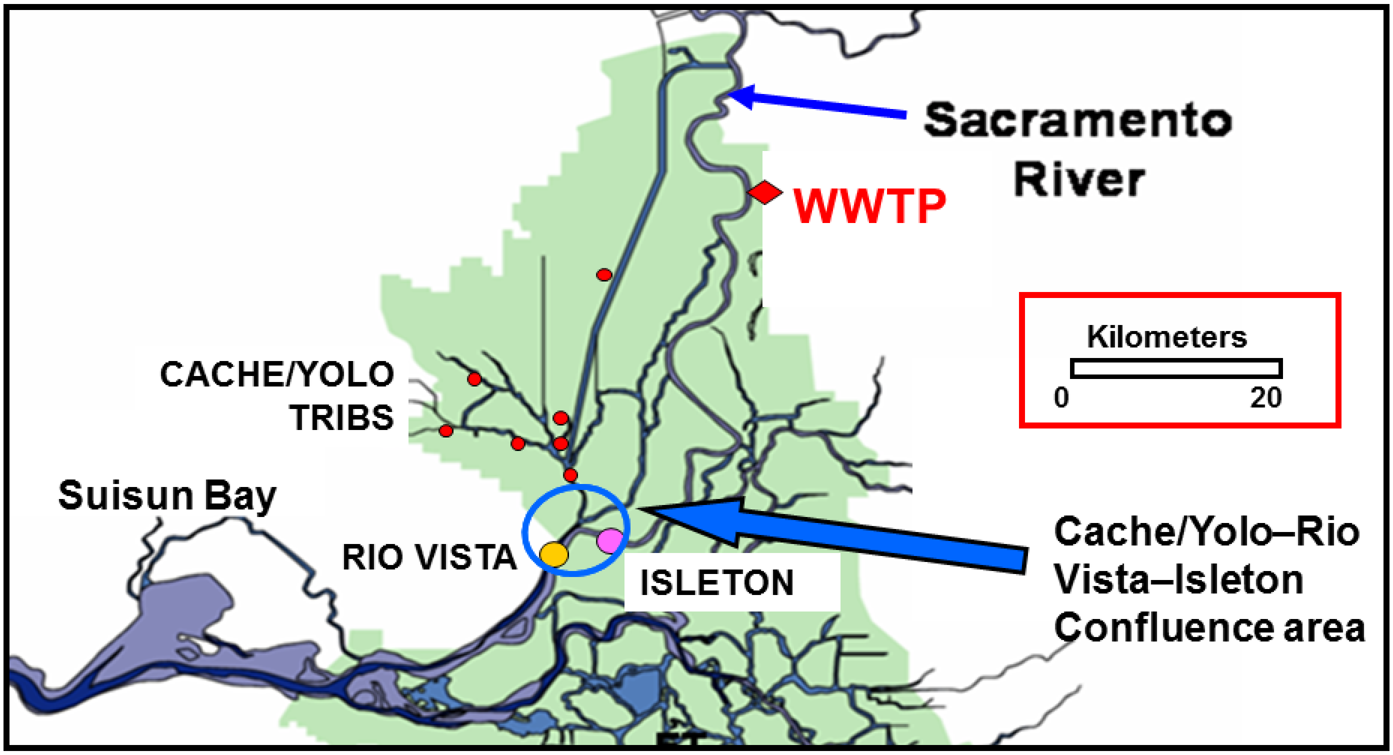

Figure 49

Locations of the sites used for the evaluation of whether mainstem Sacramento River water (as collected at Isleton, RM17) is chemically and isotopically distinctive from waters from the Cache/Yolo Complex tributaries (sloughs). If the waters are distinctive, then the data can be used to estimate the relative proportions of water, nutrients, and organics derived from the Sacramento River at Isleton and water, nutrients, and organics derived from the tributaries to Rio Vista (RM12).

Fig. 50

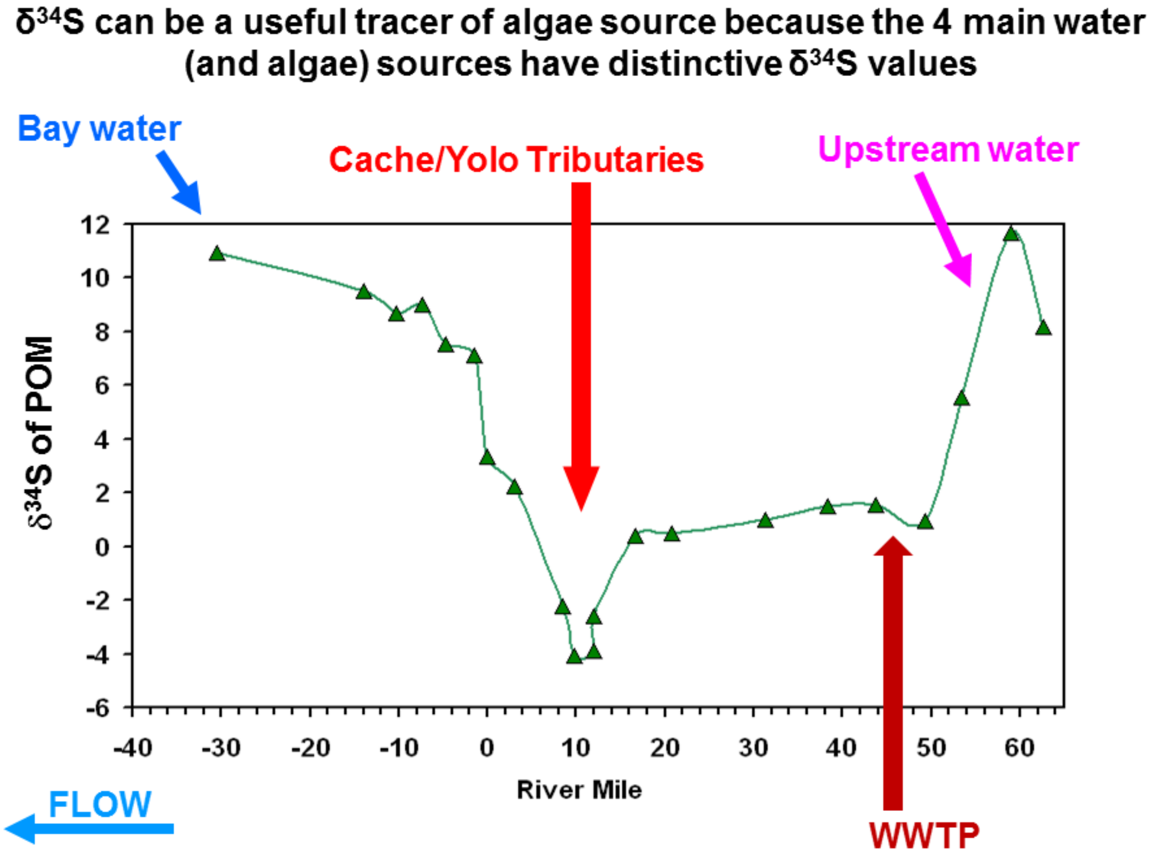

Figure 50
POM-$\delta^{34}S$ data for samples collected in April 2009 show that 4 sections of the transect have distinctive of $\delta^{34}S$ values, as noted by arrows on the plot. Effluent from the WWTP imparts a distinctive $\delta^{34}S$ value to algae growing downstream of SRWTP. The lower $\delta^{34}S$ value for POM from the Cache/Yolo tributaries probably reflects the effect of sulfur reducing reactions in upstream wetlands, and the high $\delta^{34}S$ values in the Bay show the influence of marine-derived sulfate (with a $\delta^{34}S$ of +21‰) on algae growing in the Bay. POM shows a HUGE drop near RM12, presumably due to organics from the Cache/Yolo Complex tributaries (which have very low $\delta^{34}S$ values, probably because of sulfate reduction in the wetlands). Also, effluent from the WWTP has a distinctive value compared to upstream $\delta^{34}S$ values. SO_4-$\delta^{34}S$ may be a useful tracer in this region too.

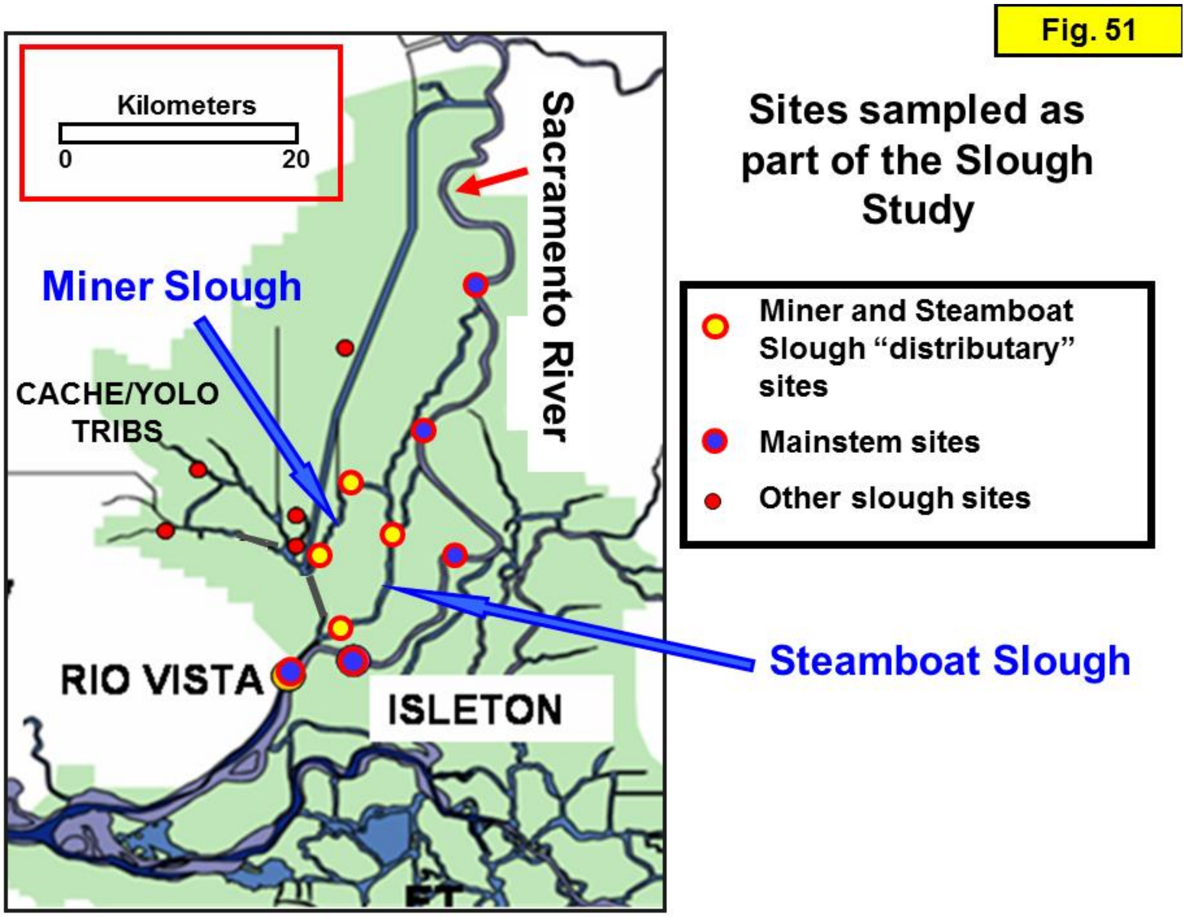

Figure 51

Locations of the sites used for the evaluation of whether mainstem Sacramento River water (as collected at Isleton, RM17) is chemically and isotopically distinctive from waters from Miner Slough and Steamboat Slough, both distributaries of the Sacramento River. The water in these distributaries is mainly derived from the Sacramento River at Courtland, but some other agricultural drainages may be seasonally important. The combined flow from Miner and Steamboat Sloughs is about the same flow as at Isleton, and they contribute roughly half the flow to Rio Vista (see Figure 52).

Fig. 52

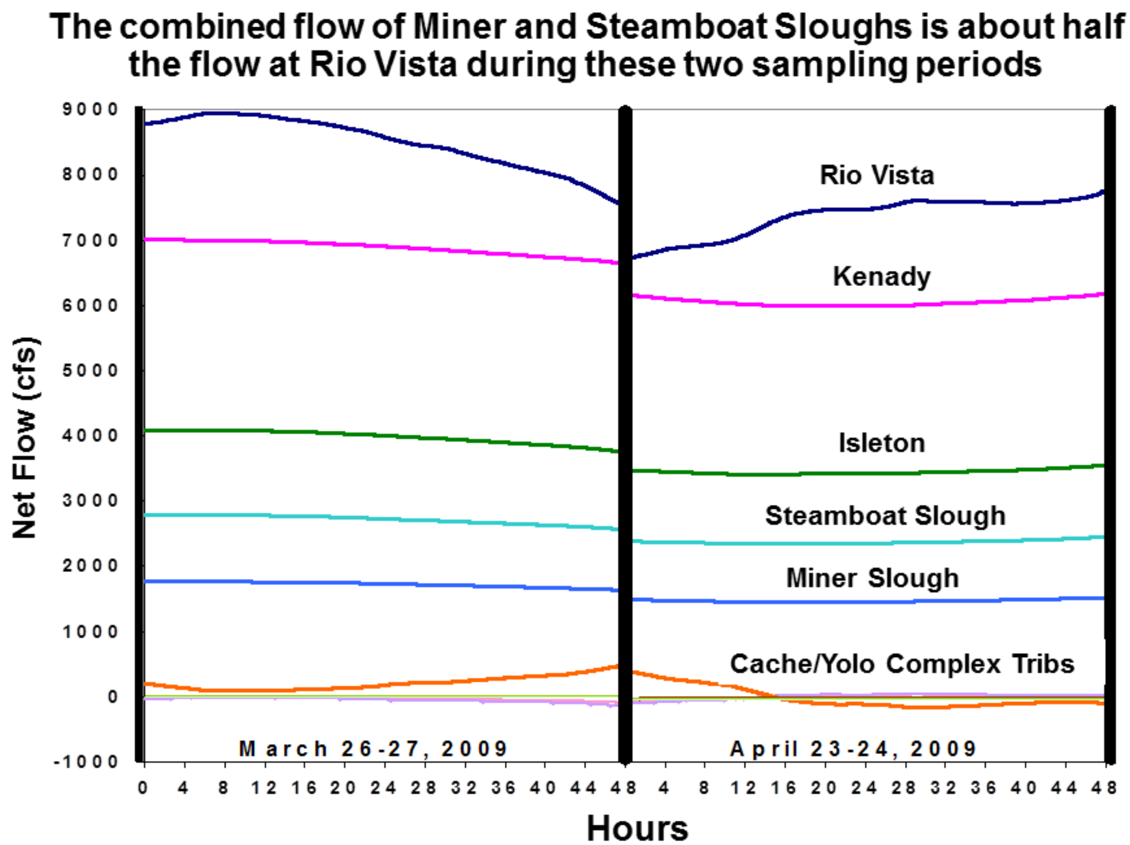

Figure 52

This plot shows the net flow values for important sites on the mainstem Sacramento River and its two main distributaries (Miner and Streamboat Slough), from Kenady (RM31) downstream to Rio Vista (RM12) during the days in March and April 2009 when isotope and chemistry samples were collected. Note that the sum of the flows for Miner Slough and Steamboat Slough is greater than the mainstem flow of the Sacramento River at Isleton, and that the flows in these two sloughs are MUCH higher than the rather trivial flows from the locations where we collected chemistry and isotope samples in the Cache/Yolo Complex tributaries.

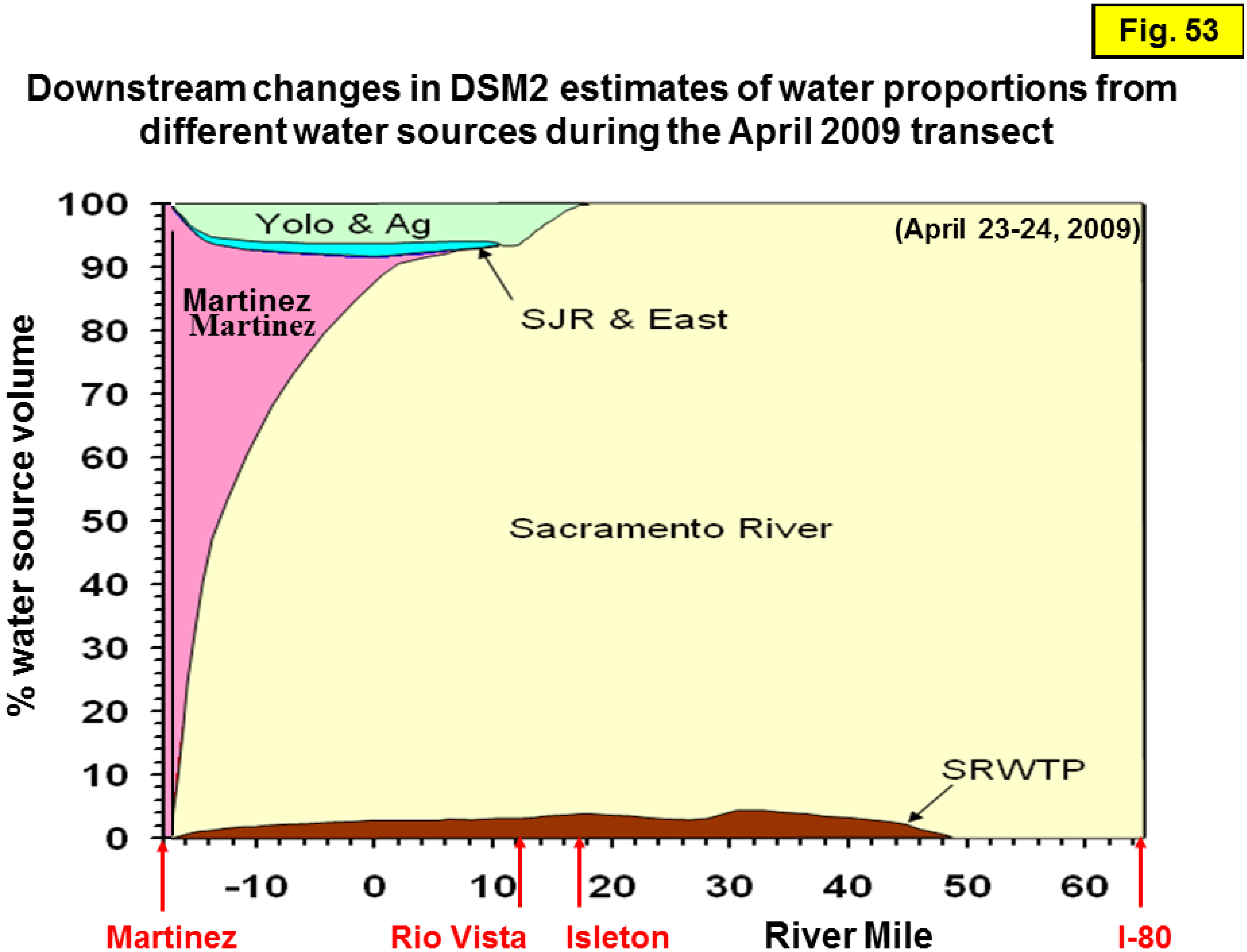

Figure 53

This plot shows how the volumetric % of water from different sources (calculated from the DSM2 model) for the April 2009 transect (April 23-24, 2009) change downstream for sites along the Sacramento River transect, from RM63 (the I-80 bridge across the Sacramento River) downstream to RM-17 at Martinez (which is as far as the DSM2 model extends). By definition, at the I-80 Bridge, 100% of the water is Sacramento River water, and at Martinez, 100% of the water is derived from downstream sources (i.e., the Bay).

Fig. 54

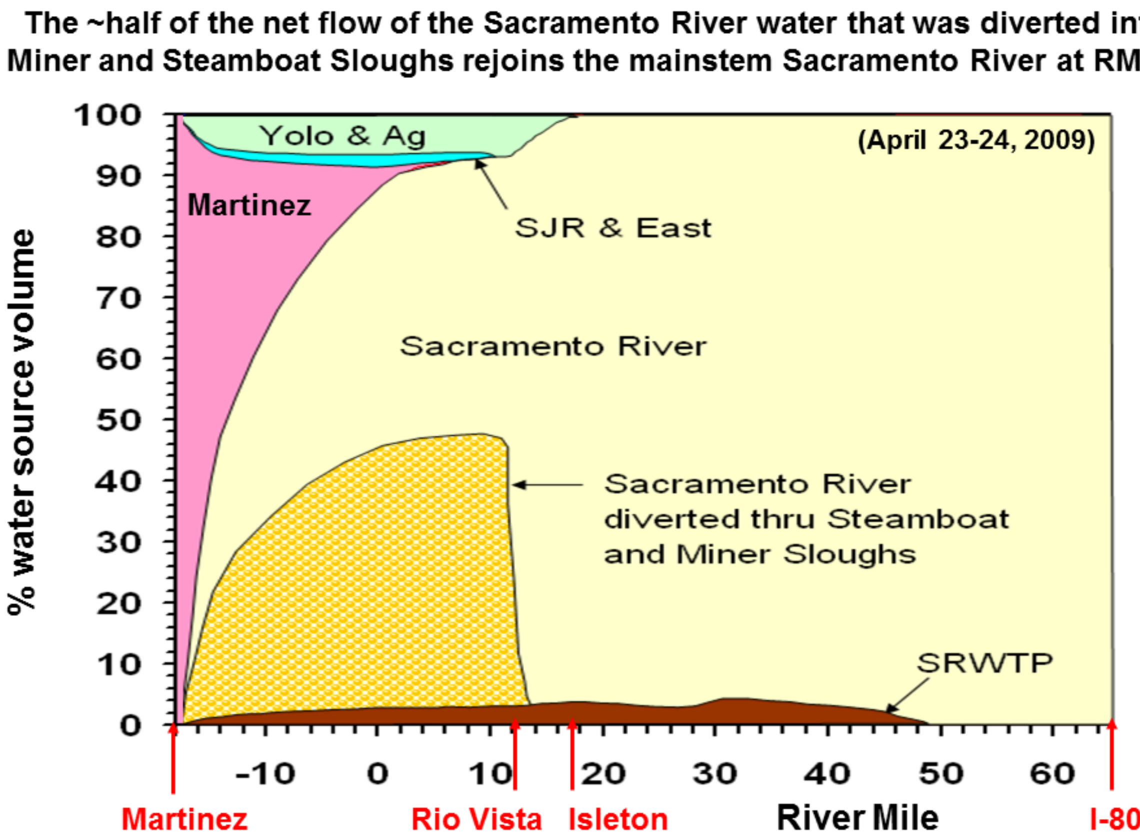

Figure 54

For this plot, the net flow values for Miner and Steamboat Sloughs for April 2009 (data for April 23-24, 2009) from the DSM2 model were used to estimate the downstream changes in the proportion of the Sacramento River water for our sampling sites that is actually diverted through these sloughs (which are actually distributaries. This plot (compared to the previous one) makes it clear that the diverted water is important volumetrically. The diverted water rejoins the mainstem at about RM14 when the Cache/Yolo Complex tributaries converge with the Sacramento River upstream of Rio Vista.